LA-UR-14-26603
Approved for public release; distribution is unlimited.

Title: Brine migration experimental studies for salt repositories

Author(s): Caporuscio, Florie Andre
Boukhalfa, Hakim
Cheshire, Michael
Ding, Mei

Intended for: Report

Issued: 2014-11-14 (rev.1)

BRINE MIGRATION EXPERIMENTAL STUDIES FOR SALT REPOSITORIES

Fuel Cycle Research & Development

Prepared for
U.S. Department of Energy
Used Fuel Disposition Campaign

Florie A. Caporuscio, Hakim Boukhalfa, Michael, C. Cheshire, and Mei Ding
Los Alamos National Laboratory

August 25, 2014

FT-14LA081803
LA-UR-14-26603

SUMMARY

Brine migration research in salt for 2014 encompassed a variety of subject matters. Two major endeavors were to continue research of 1) brine inclusion (both one and two phase) movement in a thermal gradient in multi-crystalline salt samples and 2) dehydration of hydrous silicates and sulfates in the temperature range from 50 ^{o}C to 300 ^{o}C. The water content of run of mine salt that is released by heating to approximately 100 ^{o}C was also determined. The project also examined the viability of low field Nuclear Magnetic Resonance and Incoherent Inelastic Neutron Spectroscopy as analytical tools to directly quantify the three main types of water (brine inclusions within crystals, water along salt grain boundaries, and water structurally incorporated within hydrous mineral phases) found in bedded salt deposits. All these experiments have helped to further the knowledge of brine migration in salt, especially at relatively low temperatures. Further research is envisioned for the movement of water at boundary layers of salt and clay/sulfate.

We examined water content in run of mine salt collected from current excavation operations at WIPP and determined its water content and water release at 65 and 110 ^{o}C. The experiment was performed using a gravimetric method developed in the previous year (Caporuscio et al. 2013). The results are consistent with our previous data and show that the amount of water released from salt is directly correlated to the amount of clay and other minerals contained in the salt. We also examined particle size distribution using classical sieving and gravimetric methods. We found that 65 % of the run of mine salt was between 2 mm and 9.5 mm, 25 % was > than 9.5 cm. We examined the potential utilization of low-field NMR to quantify water content in salt. The technique is highly precise, non-destructive, and provides information about the volumetric

moisture content in materials. In addition, it provides information about the binding state of water. Water contained in tight pores or associated to minerals usually gives very short relaxation times ~ 50 ms compared to free water which gives longer relaxation time ~ 300 ms. Hydration water or water associated to mineral phases gives very short relation times of ~ 10 to 50 us. We found that low-field NMR was very sensitive to moisture content in salt. The intact salt core analyzed had slightly less than 2% water which was distributed among three different main species with different relaxation times. The main fraction of water with long relaxation times of ~ 100 ms was attributed to free water. Shorter relaxation times were attributed to water associated with clay. Determination of clay content in salt could also be inferred from the relaxation of water associated with clay.

Clay and sulfate reactions with the addition of WIPP brine at hydrostatic pressure (160 bar) and elevated temperature (300 ^{o}C) indicate that corrensite clay remains the stable phyllosilicate mineral. For the sulfates, gypsum transitions to a more stable mineral phase, anhydrous anhydrite.

We also continued our examinations of brine inclusions migration in intact salt by focusing specifically on the behavior at grain boundaries and the effect of clay impurities on brine migration. We found that inclusions, (liquid only inclusions and two-phase inclusions) mobilized when the salt aggregates were subjected to thermal gradients do migrate across grain boundaries. We did not observe any migration along grain boundaries. We also found that brine migration stops when the brine intercepts clay impurities. No apparent release of moisture from the clay is observed even when the clay impurities are heated to temperatures beyond temperatures known

to induce moisture release from clay and other accessory minerals associated with salt. This is an important observation that could have very significant implications for brine migration and the mechanical properties of salt, especially when its clay content is significant.

The information gained through these investigations highlight the importance of clay and other accessory minerals for the behavior of brine contained in bedded salt exposed to thermal gradients. Our results indicate that clay content is likely to determine the moisture content of salt and its migration behavior. Our data also suggest the clay impurities in salt could act as moisture barriers and limit brine migration.

CONTENTS

FIGURES

TABLES

ACRONYMS

DI	Deionized water
DTA	Differential Thermal Analysis
FDS	Filter Difference Spectrometer
FTIR	Fourier Transform Infrared Spectroscopy
IINS	Incoherent Inelastic Neutron Spectroscopy
MRI	Magnetic Resonance Imaging
NMR	Nuclear Magnetic Resonance
RH	Relative Humidity
TGA	Thermo gravimetric Analysis
UFD	Used Fuel Disposition
WIPP	Waste Isolation Pilot Plant
XRD	X-ray Diffraction

BRINE MIGRATION EXPERIMENTAL STUDIES FOR SALT REPOSITORIES

1. INTRODUCTION

1.1 Objective

Rock salt contains small amounts of water entrapped within salt crystals (intra-crystalline), at the boundaries between salt grains (inter-crystalline),or adsorbed to the salt surface The amount of water found is salt is usually very low and can vary between 0.01 to 0.50 wt. %. In addition, rock salt contains accessory minerals (clays and sulfates), both as inclusions within salt beds, or as distinct seams, which can contain a significant amount of water. The behavior of the water contained in salt under thermal gradients is critical to the performance of salt as a medium for the disposal of nuclear waste. This is especially relevant for thermally hot nuclear waste which can mobilize water entrapped in salt. In our previous report (Caporuscio et al. 2013) we established that water content in salt was directly determined by its clay content (as inclusions) and reported on the mechanisms of brine migration in single salt crystals under thermal gradients. Our results were consistent with literature data (e.g.; Carter and Hansen, 1983) and showed that brine migrates up the thermal gradient. We also reported that at sufficiently high temperatures all inclusions become two phase inclusions in which the brine phase migrates up the thermal gradient and the gas phase migrates down the thermal gradient. We continued our examinations of brine behavior in heated salt to investigate aspects of brine migration and moisture content in multigrain salt samples. Our specific objectives for the current studies are:

1.1.1. Characterize water content in run of mine salt from current excavations at WIPP.

1.1.2. Examine the potential use of low field-NMR as a passive and more accurate way of characterizing water associated with salt. Low-field NMR, through the examination of

water relaxation times (T2), has the potential not only to characterize water content in salt, but also to determine if it is bound or free. Both salt core samples and pure clay and brine solutions were analyzed.

1.1.3. Examine the transport of brine inclusions subjected to a heat gradient. Specifically, examine the migration of brine at grain boundaries and elucidate the effect of clay impurities on brine migration.

1.1.4. To further understand hydrous mineral stability fields at elevated temperatures.

1.2 Background

1.2.1 Water content in salt

Water content in salt varies between samples and is dependent on the salt composition and the salt deposit. Literature data (Hohlfelder, 1979, Carter and Hansen, 1983) report water content that varies from thousandths of wt. % to several wt. % percent in bedded salt. Salt containing mainly halite contains small quantities of brine distributed as small intra-granular and inter-granular water inclusions. The total water content is low and is usually 0.1 to 0.5 wt. %. Inter-granular water is present in the boundaries between salt crystals and in fractures. This brine is in the form of inclusions from few microns to several millimeters in size present within the crystal structure (Figure 1). However, salt rich in accessory minerals such as clays and polyhalite contains significantly more water reaching several wt. % percent in clay rich salt (Powers, 1978, Caporuscio et al. 2013). Water associated with accessory sulfate is present as structural hydration water in gypsum, and polyhalite and as interlayer water in clays (Roedder, 1980; Roedder, 1981; Popielak, 1983, Caporuscio et al. 2013). The total water content in salt and its distribution among the three components listed above is difficult to determine and there is

significant variability among the data available in the literature. Variability in the data is mostly due to the difficulty of accurately measuring water content in each category and also due to sample heterogeneity (Roedder, 1981; Shefelbine, 1982). The quantity of water attributable to each one of the major forms of water can vary significantly within samples from the same location (Hohlfelder, 1979; Hohlfelder, 1981; Hohlfelder, 1982; Shefelbine, 1982).

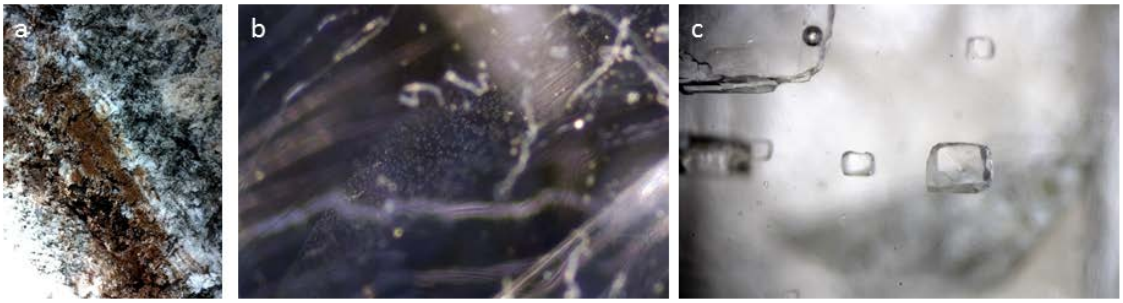

Figure 1. Picture of (a) Corrensite seam F at the WIPP repository, (b) micron size inter-crystalline water inclusions from a WIPP salt sample, and (c) mm size inclusions in a halite crystal showing both single and two phase inclusions.

Bedded salt contains a significant amount of water associated with hydrated minerals. The minerals most commonly associated with salt include oxyhydroxide minerals, carnallite ($KMgCl_3 \cdot 6(H_2O)$), bischofite ($MgCl_2 \cdot 6H_2O$), kieserite ($MgSO_4 \cdot H_2O$), gypsum ($CaSO_4 \cdot 2H_2O$), polyhalite ($K_2Ca_2Mg\ (SO_4)_4 \cdot 2H_2O$) and various clay minerals. The distribution of these various hydrated minerals in salt is highly variable and varies significantly within samples taken from the same location (Braitsch, 1971; Stewart, 1963; Sugimoto, et al, 2007; Kopp and Fallis, 1975). The amount of water associated with each mineral component can be determined theoretically from their chemical formula. In a mixture of minerals, an accurate determination of the mineralogy of the sample and quantitative measurement of weight loss under thermal treatment using techniques such as differential thermal analysis (DTA) and thermal gravimetric analysis (TGA)

or a combination of the two methods could in theory assign water releases to specific mineral phases. The amount of water contained in each mineral phase, its ease of release, and the potential for rehydration vary significantly among mineral phases. Polyhalite contains up to 6 wt. % water, clay minerals can contain between 5 and 18 wt. % water and gypsum contains up to 20.9 wt. % of water. The first and second dehydration temperature domains for polyhalite are 150-160 ^{o}C and 340 – 360 ^{o}C respectively. Clay minerals undergo dehydration between 75 and 800 ^{o}C. Gypsum undergoes dehydration between 75 to 175 ^{o}C. Carnallite, a secondary mineral phase often associated with salt and which contains up to 38.9 wt. % water undergoes dehydration between 180 and 224 ^{o}C (Smyth and Bish, 1988; Freyer and Voigt, 2003). These examples show the extent of water contained in mineral phases associated with salt and the temperature domains at which many of these phases undergo dehydration. Not only do these dehydration temperature domains overlap, there are also kinetic effects that slow reactions, thus increasing the difficulty of assigning TGA data to the various minerals and highlighting the importance of accurate quantification of water content and dehydration reaction conditions using site-specific trace minerals.

1.2.2 Incoherent Inelastic Neutron Scattering (IINS)

The processes of release and migration of confined water coupled to the thermal-mechanical behavior of rock salt have always been of concern for long-term storage. Numerous prior studies have reported the deformation and weakening of rock salt by water during long-term creep (e.g.; Urai, et al. 1986, Carter and Hansen, 1983). The authors have studied natural rock salt deformation mechanisms, by preparing thin sections of rock salt samples to exam and observe inclusion fluid behavior and brine present in grain-boundary voids using optical microscopy.

These prior studies are inadequate for three major reasons. First, the samples used in these experiments were either synthetic or changed during sample preparation. Consequently the natural complexity of the contribution of water-bearing minerals in salt to the deformation process was not addressed. Furthermore, fluid inclusions and films present at grain-boundaries were disrupted and lost. Second, the micrographic techniques (optical and electron microscopy) are only suitable to observe the presence of water and its behavior at low resolution. The behavior of confined water at the nanoscale poses are beyond the capability of these techniques. Third the efficacy in salt deformation of the three different forms of water confined in salt was not determined. The three states are: 1) Physically bound water in hydrous minerals; 2) Free water: as trapped fluid inclusions, also referred to as intra-granular water; 3) Surface water (i.e.; inter-granular water): present at grain boundaries.

To remedy these knowledge gaps, we have carried out incoherent inelastic neutron spectroscopy (IINS) studies using Filter Difference Spectrometer (FDS) to characterize the signature of water in rock salt and to investigate the liberation and behavior of confined water at elevated temperature

1.2.3 Brine migration under temperature gradients

Extensive studies examined brine migration in salt at scales ranging from cm to meters in the laboratory and under real mine settings (Machiels, 1981; Yagnik, 1982; Yagnik, 1983; Bradshaw, 1971; Krause, 1983; Nowak, 1986; Nowak, 1987; Rothfuchs, 1988). Under the influence of temperature gradients, inter-granular brine is released by a vapor transport process. This process is facilitated by the opening of the grain boundaries in polycrystalline natural salt due to the thermal stresses which accompany the thermal gradients applied to the salt (Machiels,

1981). Intra-granular brine migration in a temperature gradient depends on the nature of the brine inclusion. All-liquid brine inclusions within salt crystals migrate up the temperature gradient according to a mechanism controlled by the rate of salt dissolution at the hot face of the inclusions and to a lesser extent on the rate of salt crystallization/precipitation at the cold face of the inclusion (Olander, 1980; Olander; 1981a; Olander, 1981b, Roedder, 1980; Caporuscio et al . 2013). Inclusions are predicted to move towards the heat source because of the temperature effect on the solubility of salt. Salt will dissolve at the interface closest to the heat source and precipitate at the interface furthest from the heat source because salt solubility increases with increasing temperature (Machiels, 1981, Yagnik, 1982, Yagnik, 1983, Caporuscio et al. 2013). This process is highly dependent on the presence of imperfections and impurities in the crystal structure. Brine migration proceeds through the creation of networks of migration channels about 10 um in diameter. The chemical composition of the brine changes as it migrates towards the heat source. Impurities such as MgCl, and CaCl are precipitated and replaced by NaCl (Caporuscio et al. 2013).The rate of inclusion transport is highly dependent on the nature of the salt and the presence of impurities, and (to a lesser extent) on the rate of ion diffusion through the brine droplet, and the precipitation of salt at the cold side of the salt. The size of the inclusions does not seem to have a significant impact on brine migration.

Brine inclusions containing a gas phase have a slightly different behavior. The brine will move away from the heat source up the heat gradient similar to the behavior of brine in the full inclusion; however, the gas phase moves to the colder side of the inclusion and condenses, creating a dissolution front that moves down the temperature gradient (Caporuscio et al. 2013). This mechanism creates an internal flow that continually brings dissolved salt from the cooler

side of the inclusion to the hot side of the inclusion and water vapors from the hot side of the inclusion to the cooler side of the inclusion. These flow and evaporation mechanisms create large networks of brine migration channels that etch the inside of the salt crystals (Caporuscio et al. 2013).

The behavior of all liquid and gas-liquid inclusions becomes complicated when the inclusions reach grain boundaries, or deposits of secondary minerals associated with salt. In some studies, the migration of the inclusions was reported to continue within the adjacent grain and in other cases it ceases and the fluid spreads into micro-cracks at the boundary between grains (Carter and Hansen, 1983, Roedder, 1980). The behavior of brine that accumulates at grain boundaries is basically unknown. It is also unknown how the presence of secondary mineral phases such as gypsum, polyhalite and clay affect brine migration. Multi-scale laboratory and field studies are essential to investigate knowledge gaps in individual processes and integrate the knowledge gained at a small scale (0.10 to 10 cm) to interpret larger scale *in situ* testing studies.

2. METHODS AND EXPERIMENTAL DESIGN

2.1 Run of mine salt size distribution determination

Run of mine salt obtained from current excavations at WIPP was processed manually by sieving through different sieve sizes to determine its size distribution. The salt samples were used as received from the mine without any processing. Blocks larger than 10 cm were removed before sieving and weighed separately.

2.2 Rock salt water content characterization by gravimetric method

We examined water and accessory minerals content in rock salt samples collected from the underground salt mine at WIPP by measuring loss of weight as a result of heating. Samples were weighed, heated to the desired temperature, and weighed again until they reached a constant weight at the designated temperature. Loss of weight was attributed to water loss and the temperature was increased to higher temperature without letting the samples cool at any time during the dehydration experiment. Weighing of the samples was performed every 8 to 12 hours and total heating duration at each temperature was typically 24 to 72 hours. The dehydration experiments were performed in a heating oven equipped with exhaust valves that allow control of the oven vacuum and air circulation. The samples were gradually heated to 65 ^{o}C, and 110 ^{o}C respectively. After the completion of the heating experiment the salt samples were dissolved in water to separate the insoluble fractions, which were dried and weighed to determine their dry weight.

2.3 Dissolution and separation of the rock salt

This method is used to separate/purify non-soluble minerals from the bedded salt. In general, the salt consists mainly of halite with minor amounts of polyhalite, magnesite, clays (smectite, kaolinite), gypsum, mica, and quartz. Dissolving salt in water leads to the separation of the soluble phases, including halite and polyhalite, from the non- soluble phases. In this study, about 500 gram of salt was added into a beaker containing 1 liter distilled water and stirred gently until all coarse salt was dissolved. The suspension in the beaker was filtered using 0.45 μm filter paper. The residual of the suspension was collected on the filter paper and vacuum dried at 110 ^{0}C overnight.

2.4 Characterization of accessory minerals associated with salt using X-ray diffraction spectroscopy

X-ray diffraction (XRD) analyses were conducted on bulk salt samples, clay contained in clay Seam F, and accessory minerals associated with the orange maker bed. The samples used for bulk analyses were ground and homogenized before the analysis. Analysis of the clay component of the salt was performed on clay separated from the rock salt by dissolution of the salt component. The samples were ground and suspended in DI water to drive the dissolution salt. The supernatant was removed after saturation and replaced with fresh DI water. The operation was repeated until the clay remained suspended in solution for an extended time. The clay fraction was collected by centrifugation and was dried at ambient temperature in an open hood. X-ray diffraction (XRD) analyses were performed on a Siemens D500 diffractometer using Cu-Kα radiation. Data were collected from 2 to 70 °2θ with a 0.02 º2θ step-size and count times of 8 to 12 seconds per step. An aliquot of the < 2 μm suspension was dropped on a zero-background quartz plate and dried. This oriented mount was X-rayed from 2 to 40 °2θ at 8 to 12 s per step. Mineral identification and unit-cell parameters analysis was performed using Jade© 7.5 X-ray data evaluation program with ICDD PDF-4 database. Quantitative phase analysis was performed using FULLPAT (Chipera and Bish 2002).

Clay and gypsum dehydration phase transitions were performed using in situ X-ray diffraction characterization under controlled temperature and relative humidity. We used a Siemens D500 diffractometer equipped with an environmental cell (Figure 2) connected to a humidity generator which allows for XRD measurements to be performed under controlled conditions of RH and temperature (RH-XRD). The sample holder is equipped with a heating stage and an

external temperature controller which accurately maintains the samples temperature with +- 0.5 ^{o}C. We used this experimental setup to characterize the structural changes in the clay and gypsum under equilibrium conditions at 10 to 35 % RH at a temperature of 70 ^{o}C.

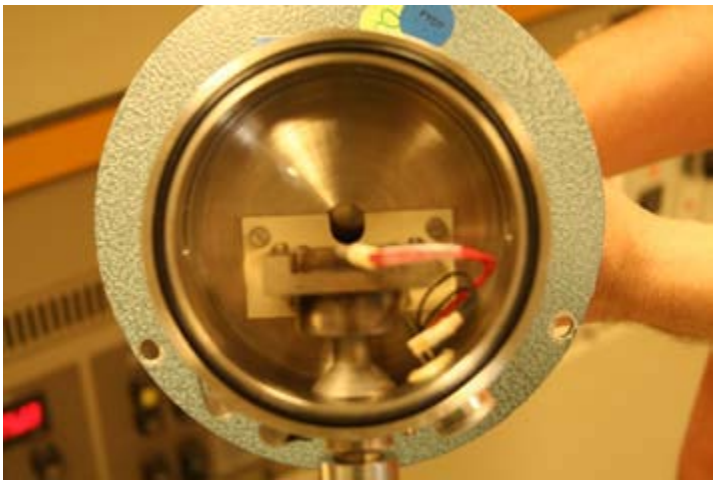

Figure 2. Bruker D8 X-ray diffractometer environmental cell. This XRD cell was used for in situ XRD examination under controlled temperature and relative humidity.

2.5 Thermo Gravimetric Analysis (TGA)

Thermogravimetry was performed on a Netzsch Jupiter STA-449 using alumina crucibles.

2.6 Incoherent Inelastic Neutron Scattering (IINS)

The Filter Difference Spectrometer (FDS) at the Manuel Lujan, Jr. Neutron Scattering Center at Los Alamos National Laboratory was used for vibrational spectroscopy with neutrons. The instrument is designed for high count rates using a large solid-angle detector. The samples are loaded into cylindrical annular aluminum sample holders that are mounted in a closed-cycle refrigerator and measured at 10K. As background for the samples, a Vanadium rod was used. For difference spectra the dried material was subtracted from the water containing samples.

2.7 Rock salt water content characterization by low-field NMR

We used a Corona low-filed NMR instrument from Vista-Calara Inc. (Figure 3) to perform measurements on salt core from WIPP. We also analyzed pure clay, gypsum, and brine under the exact same conditions to determine their relaxation times. The instrument is designed to deliver precise measurements on water content in intact samples through the measurement of the water relaxation times. The instrument uses the same physics as an MRI scanner. The sample (salt core) is inserted into the instrument opening and measurements are performed every 1.0 cm along the length of the salt core.

Figure 3. Picture showing a salt core in the measurement cavity of a Corona low-field NMR instrument.

Water relaxation (NMR echo signal is recorded following a series of pluses transmitted to the samples. Analysis of the NMR echo signal allows the determination of the samples water content (signal amplitude) and its composition (decay time). The signal amplitude gives a precise indicates the total fluid volume and its decay rate give an indication of the environment surrounding water. Water associated to tight pores gives relaxation times that are shorter than

free water. Water associated to the minerals gives even shorter relaxation times (Vista-Clara Inc.).

2.8 Brine migration in intact salt as a function of temperature

Brine inclusions migration in salt crystals were examined using a custom built setup which consisted of a heating stage, an optical microscope equipped with a digital camera, and a temperature controller (Figure 4). The salt crystals were sandwiched between two aluminum blocks with adjustable gap used to clamp the salt crystals between the two blocks. The first aluminum block is heated by an OMEGA heater fire rod with 250 W built directly into the aluminum block. The temperature of the heating block is controlled by a thermocouple and a temperature controller (J-KEM scientific model 210) that maintains the temperature with ± 2 ^{o}C of the designated temperature. The second aluminum block is not heated and equilibrates to slightly above ambient temperatures. The heating stage is mounted on Autoclaved Aerated Concrete (AAC) insulator blocks. Images of the salt crystals are captured with a Canon SLR camera coupled to an optical microscope that was used to capture still images at fixed time intervals. Transformation and migration of the inclusions is determined by analyzing the successive images captured over time.

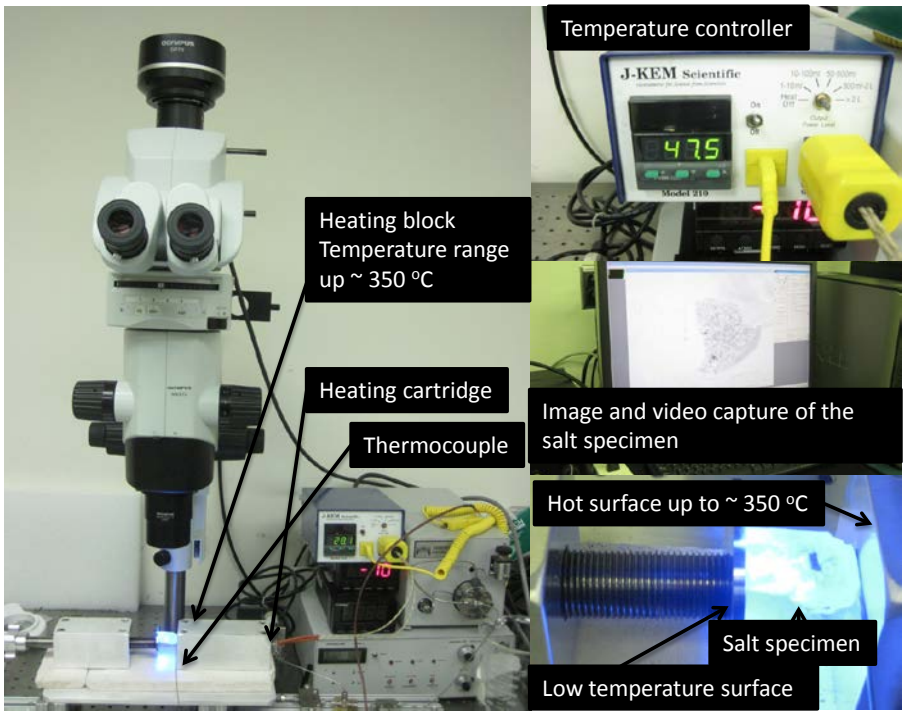

Figure 4. Temperature controlled heating stage and microscopy used for the inclusion migration studies.

3. RESULTS AND DISCUSSION

3.1 Characterization of moisture content and grain size distribution of run mine salt from the WIPP underground mine

We have previously established that water associated with accessory minerals and clay represents the largest fraction of water in rock salt. We also established a direct correlation between the clay content in salt and the amount of moisture released upon heating of salt (Caporuscio et al. 2013). In the current study we targeted the examination of moisture and accessory minerals content in run of mine salt samples collected from current excavation operations at WIPP. Run of mine salt samples were treated by heating to 65 °C and 110 °C to record their water loss according to the procedure described in the experimental design section. Clay content in the salt samples was determined by complete dissolution of the samples at the

completion of the heating experiment. The plot in Figure 5 shows the salt samples weight loss as a function of temperature and the their clay content plotted along with the data obtained previously with fresh samples collected manually at different horizons of the WIPP underground mine.

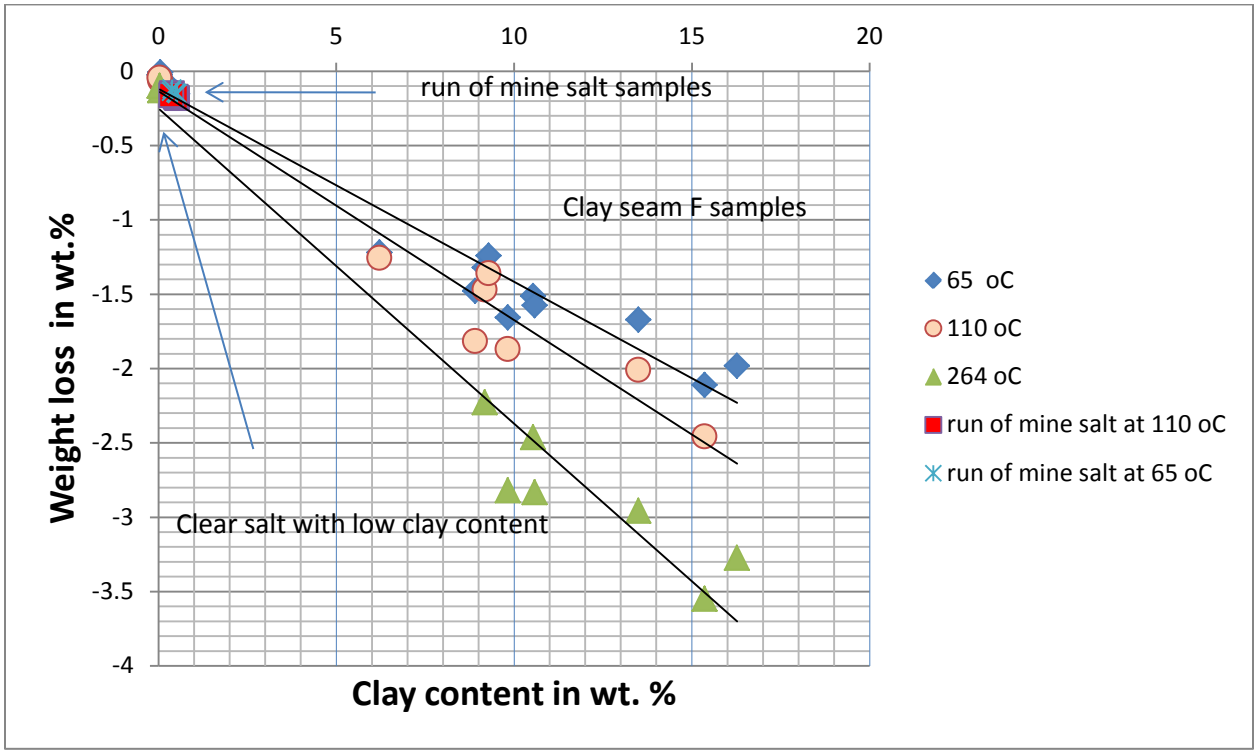

Figure 5. Plot showing a representation of salt weight loss as a function of its clay content (SDDI-SMP-00063). Data from current investigations of run of mine salt are represented by red squares. All other data points are from our previous investigation.

The data show that run of mine salt used in our experiments contained very low levels of clay and other minerals (0.44 ± 0.1 wt. %). The amount of water released from the samples did not change significantly between 65 ^{o}C and 110 ^{o}C. This is consistent with loss of any surface adsorbed water and more likely the loss of water due to clay dehydration.

We have shown previously that clay dehydration occurs between 65 and 75 ^{o}C consistent with the observation made here. The data clearly show that accessory minerals control the release of moisture from salt. The data from the current investigation shows that clay content can be used to reliably determine mobile water content in salt. It also shows that run of mine salt contains on average very low clay contents and therefore will likely contain very low levels of mobile moisture. However, the samples examined here are not representatives of all the run of mine salt that is being excavated. A more broad variation of clay content in the run of mine salt is expected, especially when the excavation horizons change. The average weight loss of the run of mine salt from samples used in our test is shown in Table 1.

Table 1. Average weight loss as function of the heating temperature for samples of run of mine salt collected from the WIPP underground mine.

Sample description	**Average weight loss at 65 ^{o}C in wt.%**	**Average weight loss at 110 ^{o}C in wt.%**
Run of mine salt	0.14 ± 0.01	0.17 ± 0.01

We have also performed a size distribution analysis of the run of mine salt samples used in our experiments. The experiment was performed by sieving a 10 gallon salt drum through different sieve sizes and determining the mass of each size fraction. The data in Figure 6 show the size fractionation of the run of mine salt used in our experiments.

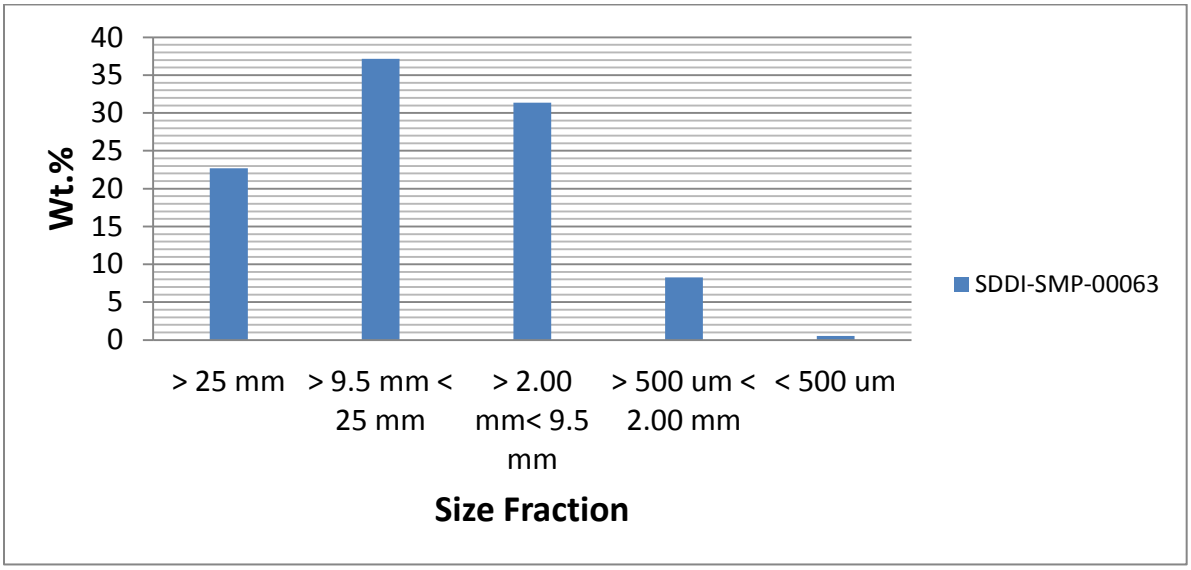

Figure 6. Plot showing the size fractions of a run of mine salt sample used in our experiments. The sample was collected from current excavation operations at the underground mine at WIPP (SDDI-SMP-00063).

3.2 Thermogravimetric analysis of accessory mineral associated with WIPP salt

We carried out thermo gravimetric analysis (TGA) for two salt samples to determine changes in their physical and chemical properties as a function of increasing temperature. The TGA results of these two samples are presented in Figure 7.

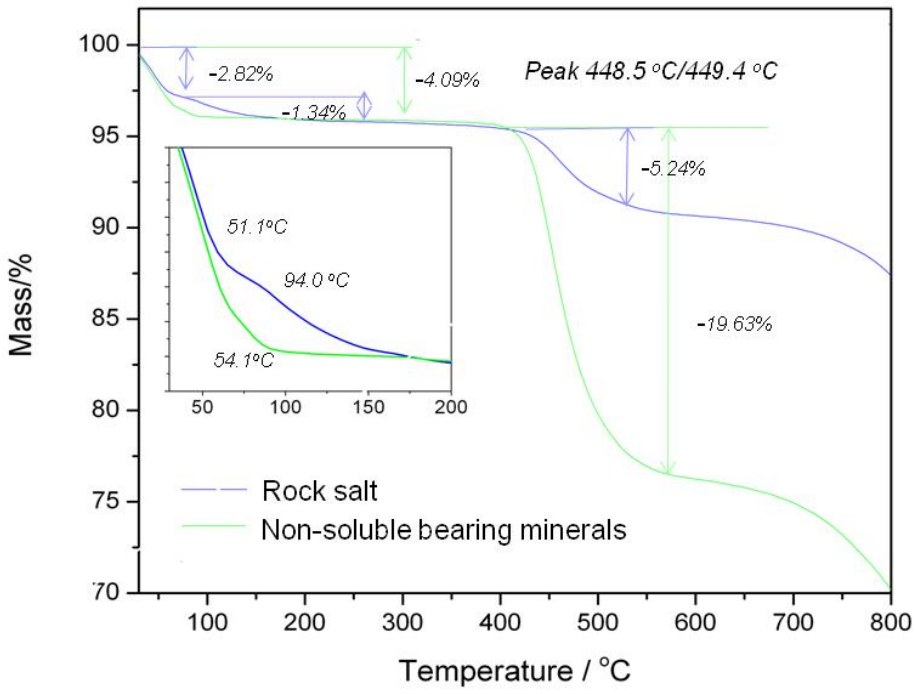

Figure 7. TGA analysis of rock salt and non-soluble minerals from rock salt.

TGA analysis suggests that there are two weight loss scenarios for the non-soluble minerals. One occurs between room temperature and 54.1 ^{o}C with a weight loss of 4.09 weight %, the other at 449.4 ^{o}C, with a weight loss of 19.63 weight %. The observed weight loss from 54.1 ^{o}C to 65 ^{o}C is likely due to loss of interlayer water in the clay. The observed weight loss at 449.4 ^{o}C is attributed to a phase change of the clay. However, no structural characterization was performed to determine the nature of the structural changes that occurred, as these transformations occur at much higher temperatures than is expected in repository setting.

Rock salt showed three weight loss stages: the first occurred between room temperature and ~ 94.0 ^{o}C, the second between 94.0 ^{o}C and ~ 150 ^{o}C, and the last at ~450^{o}C. We expected two

other forms of water in rock salt, i.e., free water as fluid inclusion and surface water confined in grain boundaries. In comparison to the result of the non-soluble bearing minerals sample, the weight loss between 51.1 ^{o}C and 150 ^{o}C may be attributed to kinetically hindered loss of interlayer water in clay and sulfate dehydration reactions. Similarly, the weight loss at 448.5 ^{o}C is due to loss of bond/structure water present in the minor amounts of non-soluble minerals resulting in phase changes from clay to mica.

3.3 Incoherent inelastic neutron spectroscopy investigation of confined water

We have carried out incoherent inelastic neutron spectroscopy (IINS) studies using Filter Difference Spectrometer (FDS) to characterize the signature of water in rock salt and to investigate the liberation and behavior of confined water at elevated temperature.

FDS neutron spectroscopy (a vibrational spectroscopy using inelastic incoherent neutron scattering) is of particular use in sampling protons. As such, the librational modes of water, which are either weak or inactive in optical vibrational spectroscopy (e.g., Raman or FTIR), are easily observed with neutrons. Furthermore, the scattering intensity correlates with amplitude of motion. As water librational motions have large amplitudes, the librational signal is extremely intense in the neutron vibrational spectrum. These liberations also tend to be very sensitive to the molecular environment of water (hydrogen-bonding, surface water, binding to cations). The librational signature is therefore considered to be a powerful technique to investigate the nature of water in materials (Line and Kearley, 2000).

Our principal result shows pronounced spectroscopy features within the librational modes of confined water in rock salt occur between 300 and 1100 cm^{-1}. With increasing temperature these

features become less intense. The results also show that spectroscopic signature of hydrous minerals in rock salt within the librational modes between 300 and 1100 cm^{-1} differs distinctively from that of confined water in rock salt. These results are pertinent because they are obtained in situ, without subjecting rock salt samples to any sample preparation. This study suggests that FDS may in the future be a viable diagnostic method to fingerprint and quantify the behavior and movement of water present in salt and hydrous minerals.

Two samples were used in this study. One is Permian rock salt located near Carlsbad, New Mexico. The rock salt from the field is minimally destructed and processed, representative of the heterogeneous nature of the field sample. We anticipate that water in the rock salt sample is present in three forms: 1) free water trapped as fluid inclusion in salt crystals; 2) surface water in grain boundary; and 3) bond/structure water in hydrous minerals. The second sample consists of non-soluble minerals present in rock salt. The sample of non-soluble minerals was obtained using dissolution and separation of the rock salt, as described previously. We expect that the water in the sample of non-soluble minerals is bond water only.

3.3.1 IINS spectra of rock salt and non-soluble minerals in rock salt at room temperature

FDS spectra of the rock salt and the non-soluble minerals in the rock salt are presented in Figure 8. As shown in Figure 8, pronounced spectroscopic shifts within the intermolecular liberation modes occur between 300 and 1100 cm^{-1}, suggesting that FDS could be a diagnostic tool capable of identifying free water vs. bond/structure water.

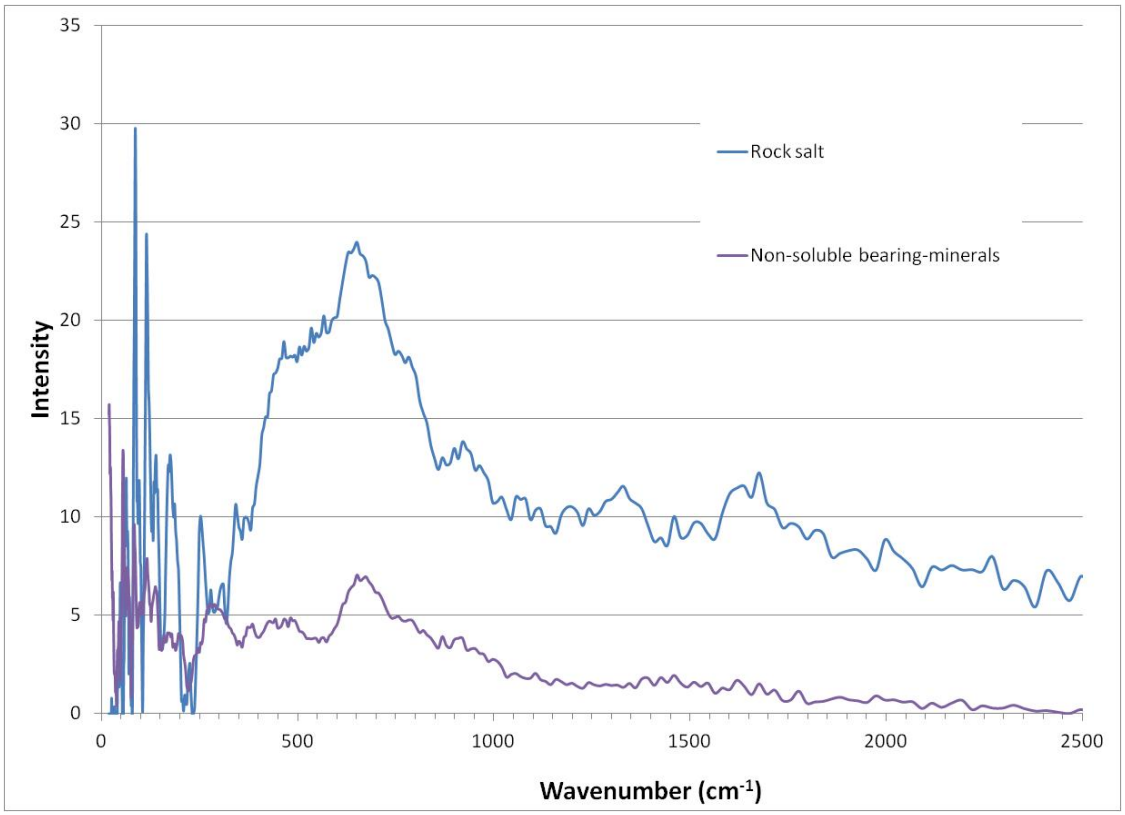

Figure 8. IINS spectra of the rock salt and the non-soluble minerals in rock salt.

FDS measurement results of rock salt as a function of temperature are presented in Figure 9. As temperature increases, the vibration mode spectroscopic features of free water decrease in intensity, between 300 to 1100 cm^{-1}. Figure 9 also shows that at 150 ^{o}C, virtually all free water is released from the system.

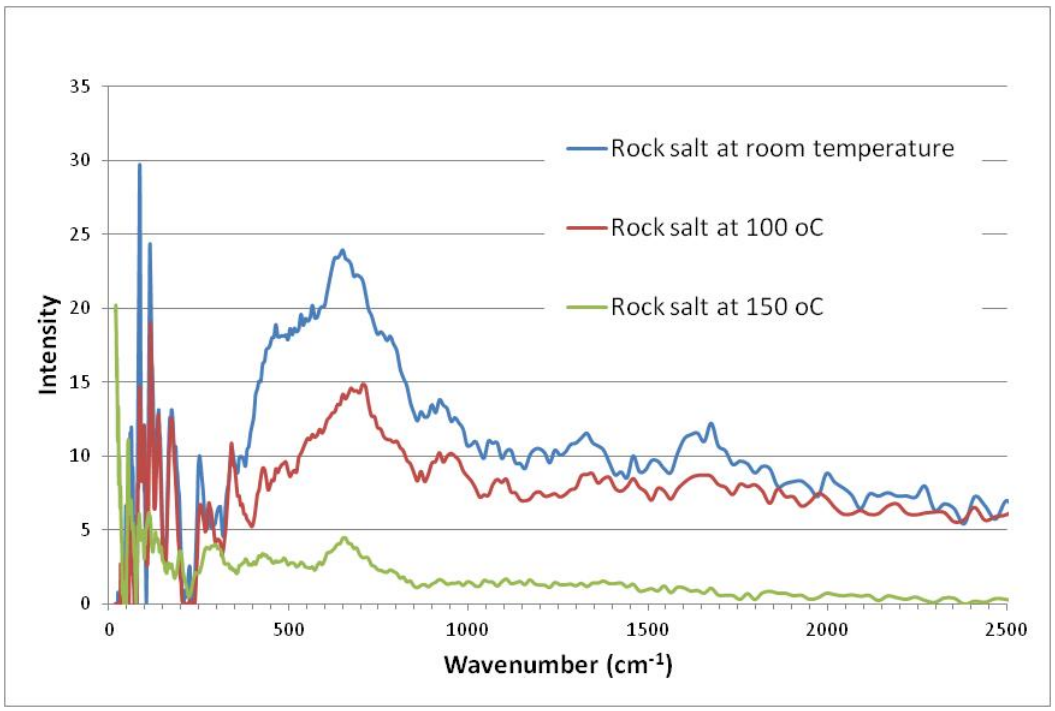

Figure 9. IINS spectra of rock salt as a function of temperature.

3.3.2 IINS spectra of minor phases at elevated temperature

FDS measurement results of the non-soluble minerals in rock salt as a function of temperature are presented in Figure 10. The spectroscopic features at 450^{o}C differ significantly from those at low temperature, indicating the occurrence of a structural change, resulting in phase changes.

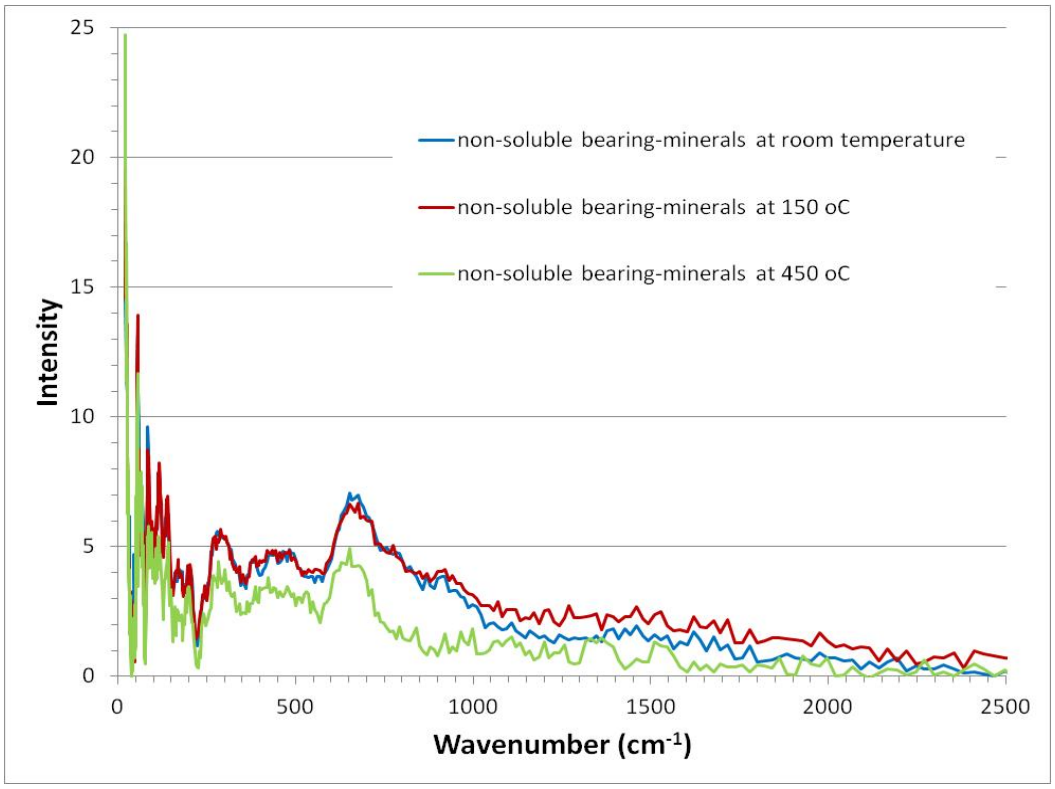

Figure 10. IINS spectra of the non-soluble minerals separated from the rock salt as a function of temperature.

3.3.3 Application of low-field NMR for the characterization and quantification of water content in intact salt

NMR is known to be one of the most versatile techniques for measuring moisture content in solid materials. It has been applied for the measurement of moisture content in wood, biofilms, soils, and may other materials (Vista-Clara Inc.). The technique is highly precise, non-destructive and provides information about the volumetric moisture content in materials and provides additional information about the binding state of water. For this project we used a commercial instrument (CORONA, manufactured by Vista-Clara INC.) and an in-house built low filed NMR instrument to explored the potential application of the low-field NMR technique for the quantitative determination of water content in WIPP salt (and its classification among the different components of water that are usually associated with salt) inter-granular, intra-crystalline,

adsorbed water, and hydration water associated to clay minerals. Typically the sample is placed in the sample bore which is surrounded by magnets which cause the magnetization of the hydrogen nuclei in the water. A series of radio frequency pulses are applied to the samples and the resulting NMR echo signals from the fluid are recorded. The signal amplitude is indicative of the quantity of hydrogen containing molecules (water for our salt samples) and the decay behavior of the echo signal (T2) is indicative of the water environment. A pure water sample typically gives a mono exponential decay characterized by a decay time typically in 200 to 400 ms. Mixtures of water species with different environments give multi-exponential decays that are parameterized by the relaxation times of the different water species. Figure 11 shows an NMR echo signal and its numerical fit using a multi-exponential decay. The plots show that the salt core contains about 1.98 volumetric % of water of which 0.9 % is characterized with a very short relation time of ~3/10 ms, usually associated with structural water or hydroxyl groups associated to the mineral structure. Two other species with higher relaxation times 30 to 300 ms are also observed and are attributed clay interlayer water and free water respectively.

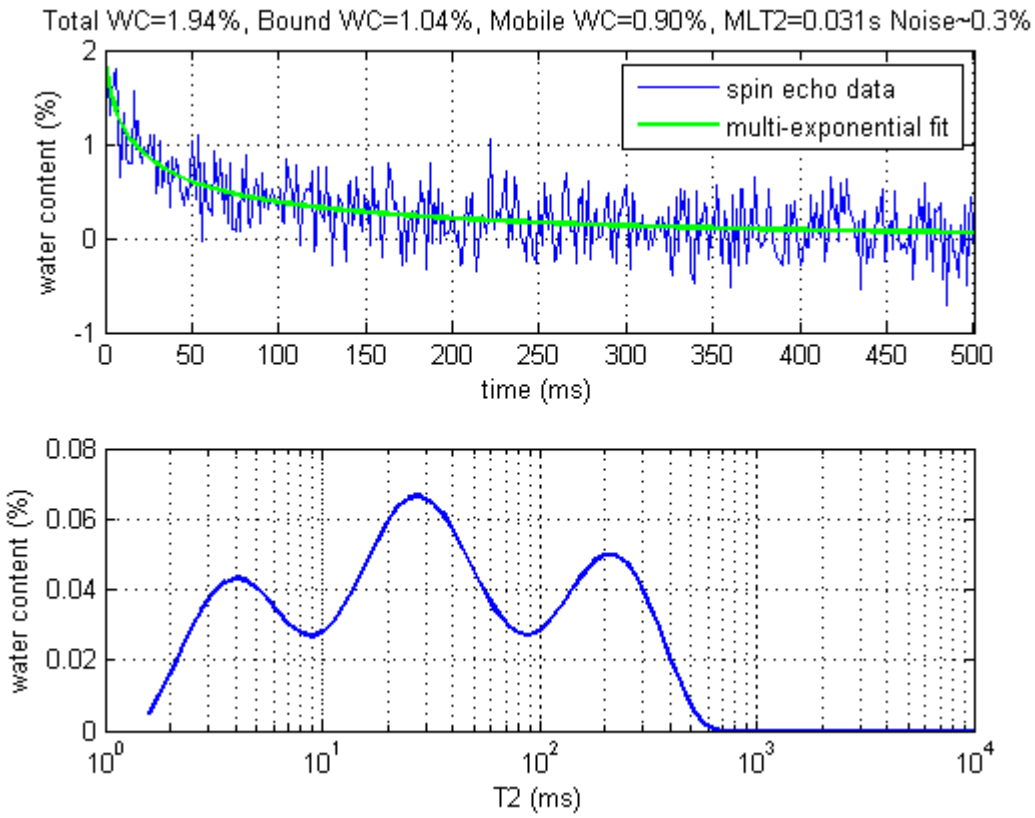

Figure 11. NMR echo signals and multi-exponential relaxation-time distribution for a salt core from WIPP. We distinguish three separate water components with relaxation times of ~3 ms, 30 ms, and 200 ms.

The data in Figure 12 show the echo signal and the multi-exponential relaxation-time components obtained for saturated clay sample collected from WIPP. Analysis of the echo signal decay over time shows the presence of two district water components with relaxation times of ~ 2 ms and 70 ms. These relaxation times are tentatively attributed to the clay interlayer water and hydroxyl groups of the clay structure.

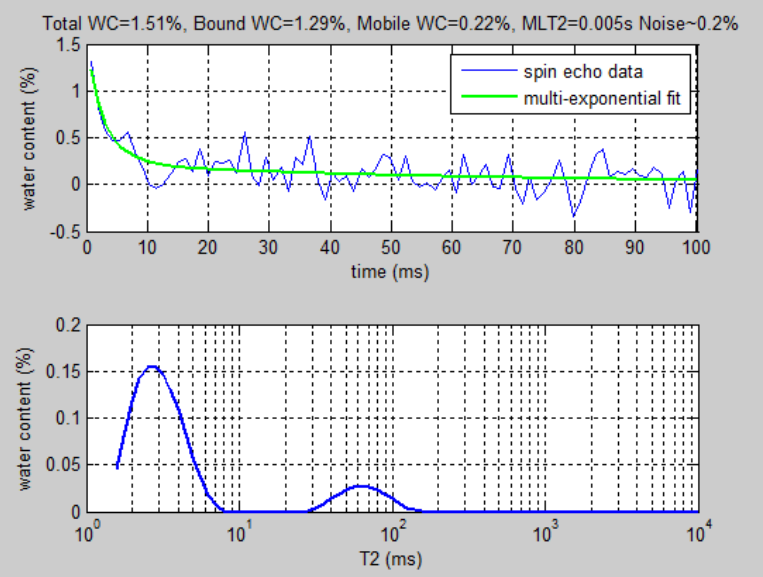

Figure 12. NMR echo signals and multi-exponential relaxation-time distribution for a saturated clay sample from WIPP. We distinguish two separate water components with relaxation times of ~2 ms, and 70 ms. These two water components are attributed to structural water or hydroxyl groups associated with the clay structure and to the inter-layer water.

The preliminary data obtained using low-field NMR for the quantification and characterization of water present is salt show that this technique is very sensitive to water content and can easily measure moisture content of ~ 0.2 %. It also provides a qualitative and quantitative determination of the bound versus mobile water, which can be attributed to the different water components associated with salt (free water, hydration water etc.).

We used low field NMR to map an intact salt core from WIPP. The core was mapped for water content by performing measurements every 1 cm of the salt core. The water content and its distribution among different fractions with different motilities are shown in Figure 13. The echo data were analyzed to determine noise level and level of averaging required to reduce the noise before signal analysis. Averaging of the echo signal every 3 cm was performed for the length of

the salt core (29 cm). The eco signal varied with the salt position in the instrument which is reflective of the variability of the water environment within the salt core. The data in Figure 13 show signal and numerical fitting at the 14 cm position along the length of the salt core.

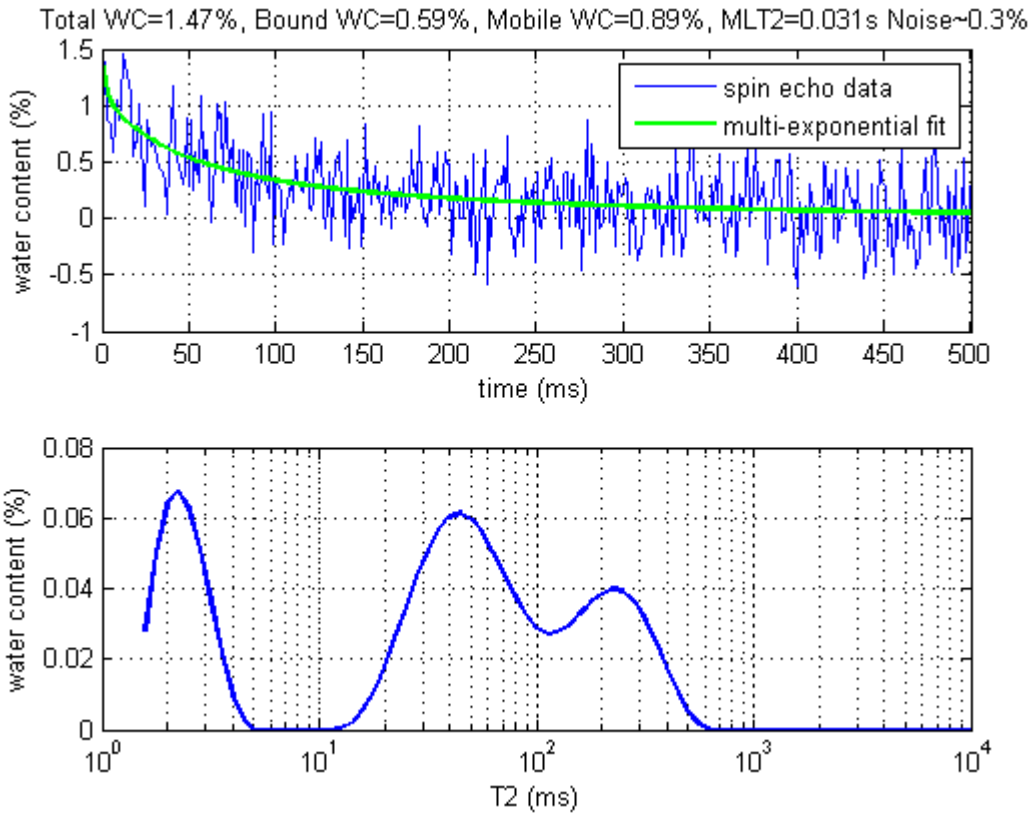

Figure 13. Plot of eco signal and numerical fitting of the decay signal for two discrete positions at 14 cm of the salt core. Data acquired using 1200 averages. We distinguish three separate water components with relaxation times of ~2 ms, 50 ms, and 200 ms.

The data show that that water content in the salt core is consistent and is slightly less than 2 wt. %. However, the speciation of water changes significantly from one position to another. A representation of the water content and its attribution to free and bound water obtained by averaging the signals obtained for every 3 cm is presented in Figure 14.

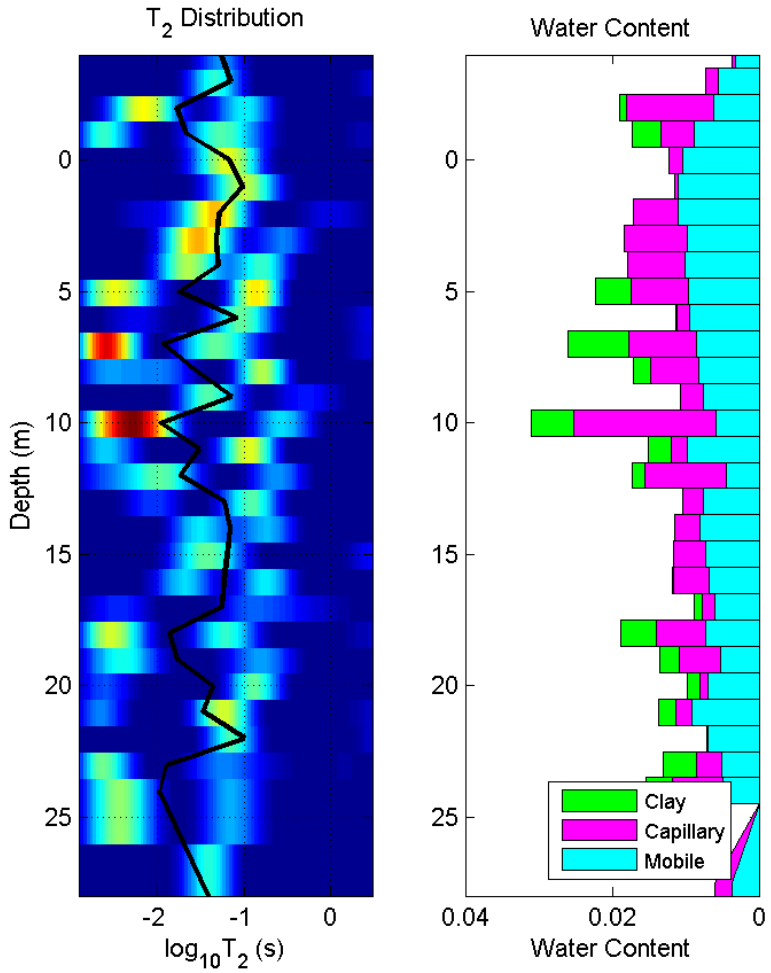

Figure 14. Figure showing the distribution of the relaxation time T2 obtained at discrete 1 cm position (average of every 3 cm) for salt core obtained from WIPP (left) and the attribution of water content to free water, water associated to clay and water present in the salt micropores.

When we increase the level of averaging (every 6 cm) the resolution of T2 and nature of water are reduced allows distinction of areas with high clay content in the salt core (Figure 15).

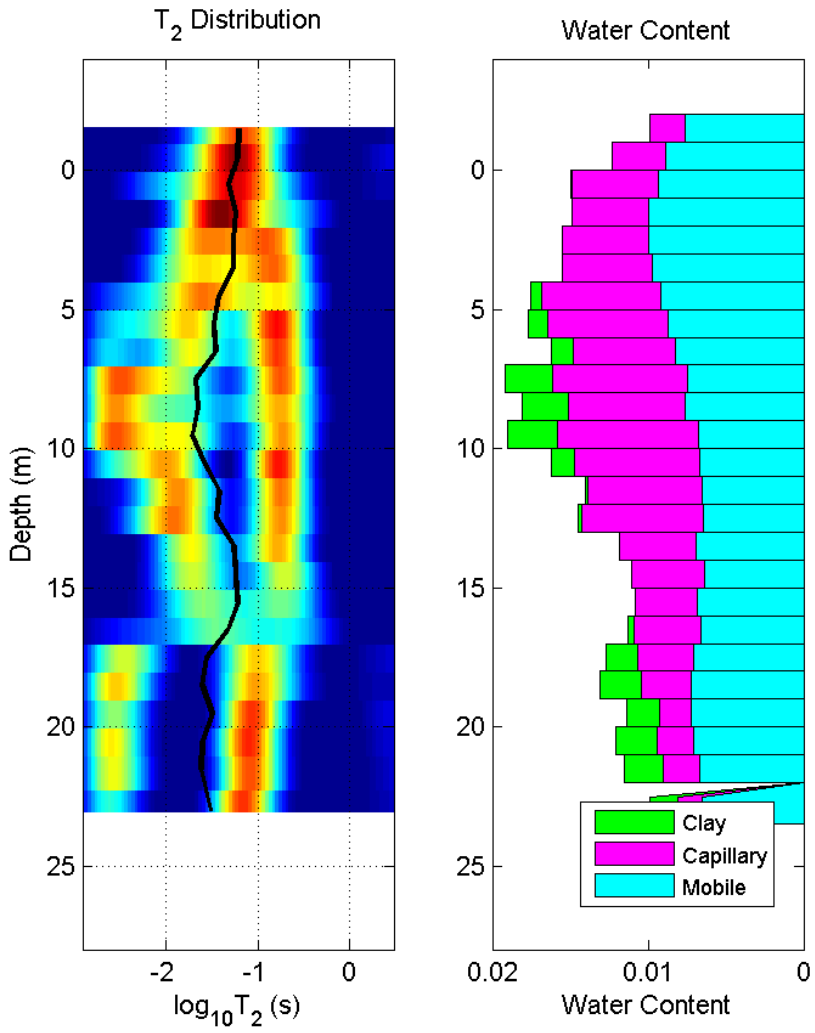

Figure 15. Figure showing the distribution of the relaxation time T2 by average data every 6 cm.

The lower resolution of the mapping allows the distinction areas with very short relation times (~ 30 to 70 ms) attributed to interlayer water associated with clay minerals. The longest relaxation times ~ 200 to 300 ms which was consistent with the relaxation time obtained for saturated brine are attributed to free water present in salt. Shorter relaxation times of 2 to 10 ms observed are attributed to the presence of structural water or hydroxyl groups associated to the accessory minerals present in salt.

These preliminary data are encouraging and show that low-filed NMR can be applied to determine the moisture content in salt with high accuracy. This nondestructive technique also allows the determination of the distribution of water among the different water species associated

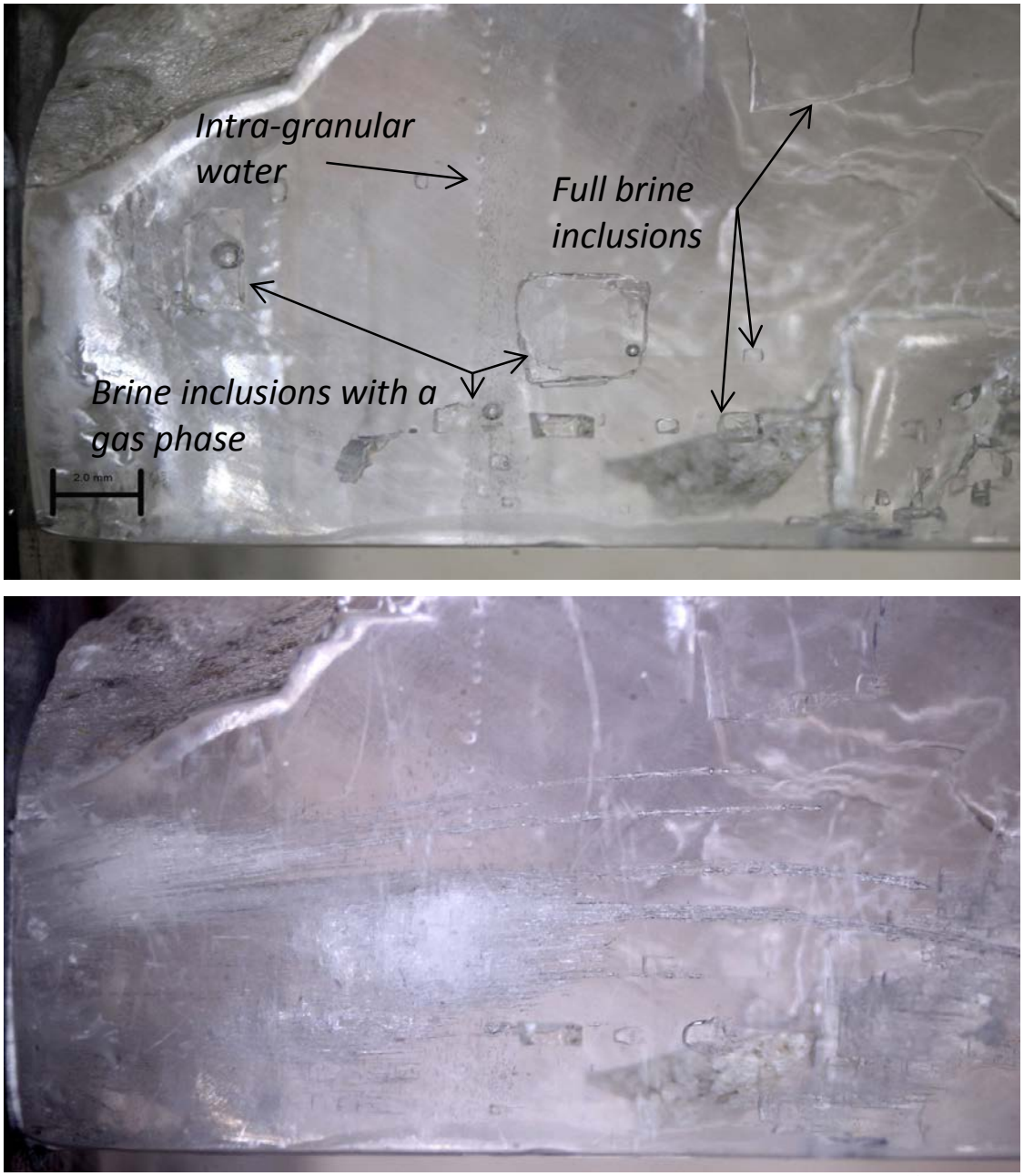

Figure 16. Picture showing a salt crystal before (top) and after heating at 240 ^{o}C for about 3 weeks.

with salt (free, bound). However, more calibrations are needed to retrain the relaxation times for each water components and define how impurities dissolved in water affect its relaxation time under the low filed conditions used by the instrument.

3.4 Laboratory examinations of brine inclusion migration in a multi-crystalline salt under a thermal gradient

In our previous report (Caporuscio et al. 2013) we presented results on brine inclusion migration in intact single salt crystals subjected to thermal gradients. The results detailed the behavior of individual brine inclusions (one phase and two phase inclusions) in a thermal gradient. Our data indicated that both types of inclusions (liquid only and two-phase inclusions) were mobilized when the salt crystals were subjected to thermal gradients. More importantly we were able to show that moderate temperature of as low as 40 ^{o}C and a temperature gradient of a few degrees were sufficient to mobilize brine contained in salt. Under low temperatures (temperatures below the temperatures necessary to create a vapor phase in the inclusions) the brine migrates up the thermal gradient through a network of narrow migration channels. The composition of the brine changes from the original brine which contained Na, Ca, Mg, Cl and SO_4 to saturated pure NaCl brine (Bein, et al., 1991).

Multiphase inclusions or inclusions that are heated to the point where a gas phase is created do migrate in both directions. The liquid phase migrates up the thermal gradient and the gas phase migrates down the thermal gradient (Anthony and Cline, 1971, 1972). We also found that gas phase migration is much faster than liquid brine migration. At sufficiently high temperatures (T> ~160 ^{o}C) all inclusions became two-phase inclusions, in which brine migrated up the temperature

gradient and the gas phase migrated down the temperature gradient. The rate of the brine migration was found to be dependent on the amplitude of the thermal gradient, the temperature of the hot face of the inclusion, and to a lesser extent on the size of the inclusion. The data showed that brine migration could significantly alter the mechanical properties of salt Figure 16 illustrates a single salt crystal before and after heating, showing a significant degree of crystal etching in the salt exposed to a thermal gradient.

Current efforts focus on the examination of brine migration in multi-crystalline salt specifically we examined the behavior of brine migration at the grain boundaries and when brine migration intercepts accessory minerals or clays.

3.4.1 Brine migration in pure multi-crystalline salt under a thermal gradient

Measurements were performed on multi-grain salt specimens cut from a salt core collected from WIPP. The salt core was cut (using a wire cutter) into sections that are few cm thick. These sections, which contained a significant number of brine inclusions, were prepared for mounting in the microscopy heating stage by further resizing to the proper dimensions. The multigrain salt was heated by contacting one of the salt sides to a heating block heated to 138 ^{o}C. A temperature controller was used to maintain the heating block at a constant temperature. A constant temperature gradient was established through the salt specimen within one hour and remained stable for over a month. Temperatures at the surface of the salt measured using a thermocouple at different distances form the heating block are shown in Figure 17.

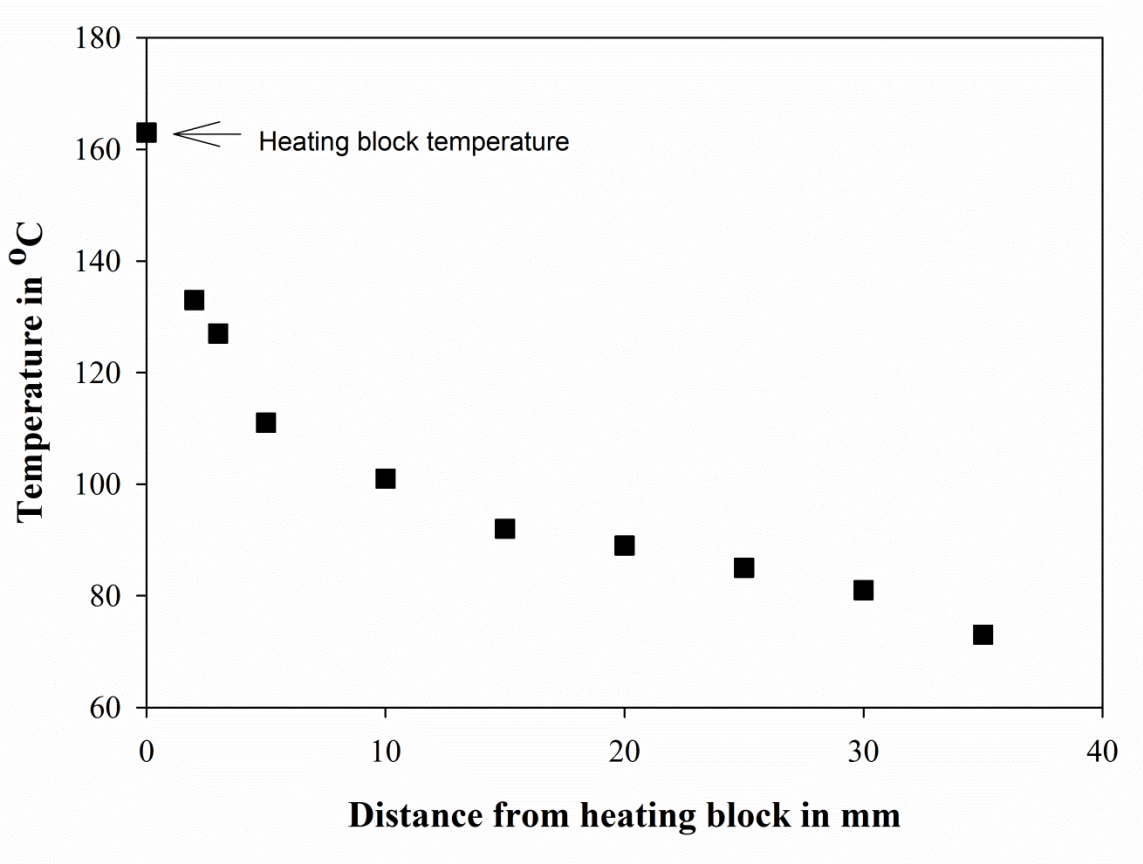

Figure 17. Plot of temperature profile in a multigrain salt used to examine brine inclusions behavior at grain boundaries. Conditions: Salt dimensions: length: 4.5 cm, width 3.5 cm. Temperature of the heating block: 163 ^{o}C, temperature of the salt in contact with the heating block = 138 ^{o}C, Temperature of the room = 25 ^{o}C

The temperature profile in salt is consistent with our previous observations and shows a lack of coupling between salt and the heating block, which results in a temperature drop of about 20 ^{o}C between the heating block and the surface of the salt in contact with the heater. The temperature decreases exponentially in the direction away from the heat source.

The salt specimen used for these experiments has many small brine inclusions distributed throughout the different crystal grains (Figure 18). The approximate percentage of inclusions ranges from 0.5 to 7 volume % the size of all inclusions was less than 1 mm long.

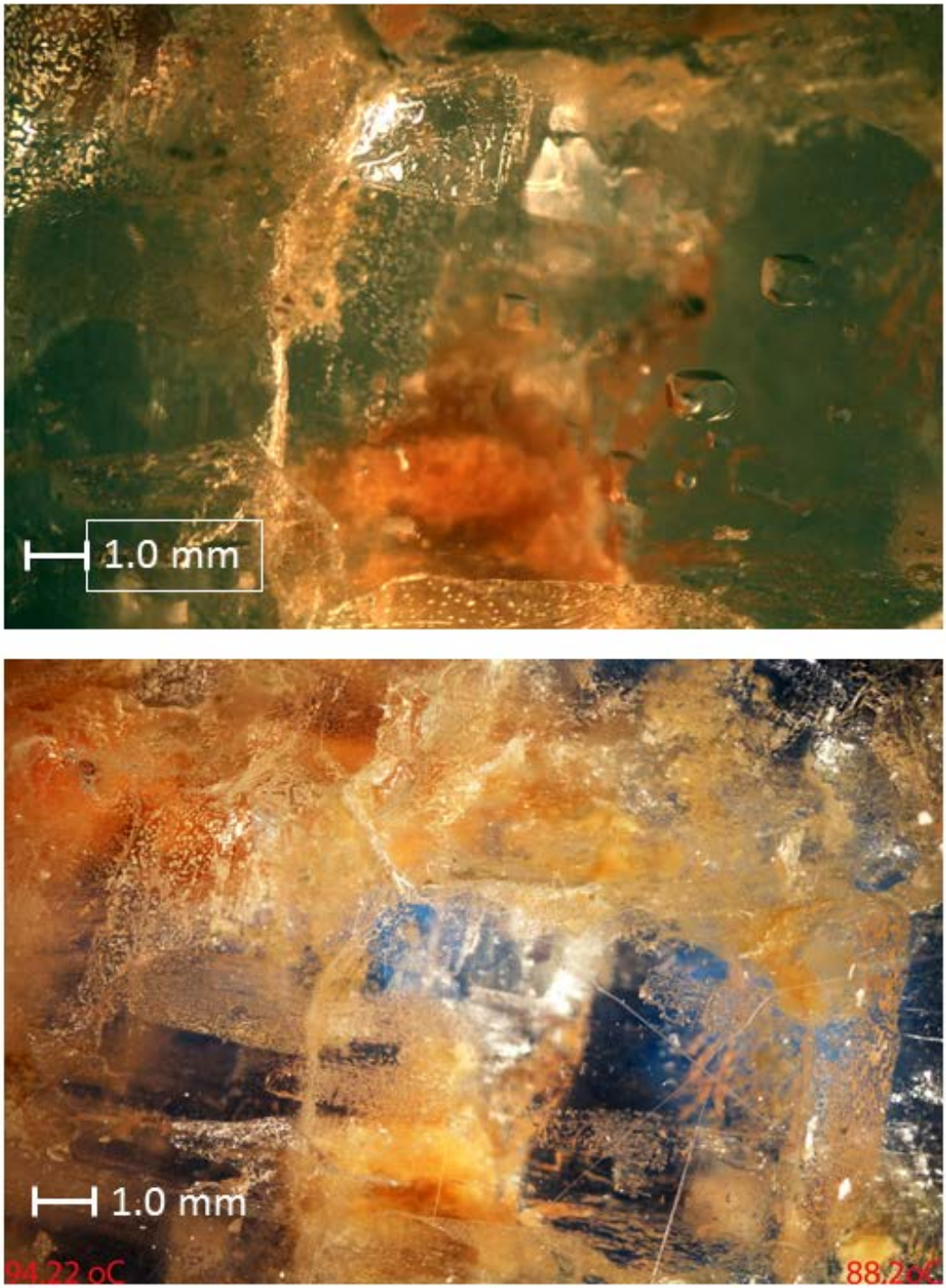

Figure 18. Picture showing a salt specimen used to examine brine behavior at grain boundaries. (Top) initial salt specimen (bottom) salt specimen following exposure to a thermal gradient for 427 hours.

Following exposure to a heat gradient of 10 ^{o}C/cm for an extended time (427 hours), all inclusions of all sizes moved progressively toward the heat source. The inclusion migration was consistent with the results reported in our previous report. Temperature and the temperature gradient were the most significant parameters affecting the rate of brine migration. All inclusions crossed the salt grain boundaries independent of their size or orientation at the grain boundary.

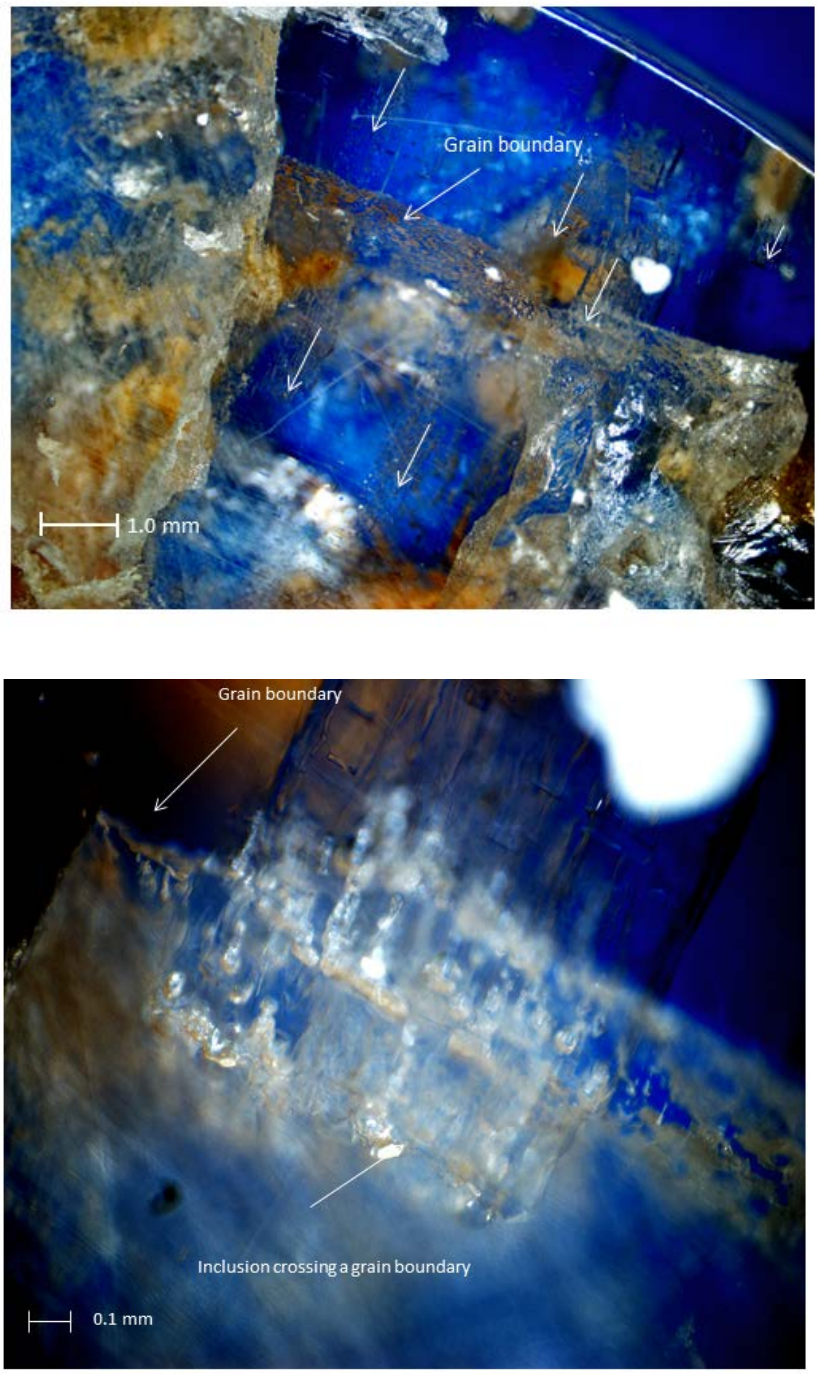

Figure 19. Images showing multiple inclusion crossing grain boundaries, arrows show the migration direction of the expanded inclusions (top) and a single inclusion crossing a grain boundary (bottom).

The images in Figures 18 and 19 shows several inclusions captured crossing grain boundaries. We did not observe any moisture migration along grain boundaries. This is usually easy to detect and is reflected by the deposition of salt effloresces at the salt surface or the grain boundaries.

The rate of brine migration was also consistent with our previous observations. The data in Figure 20 represent a plot of brine migration velocity plotted for several inclusions as a function of time. The data show that the size of the inclusions does not influence the velocity of brine migration.

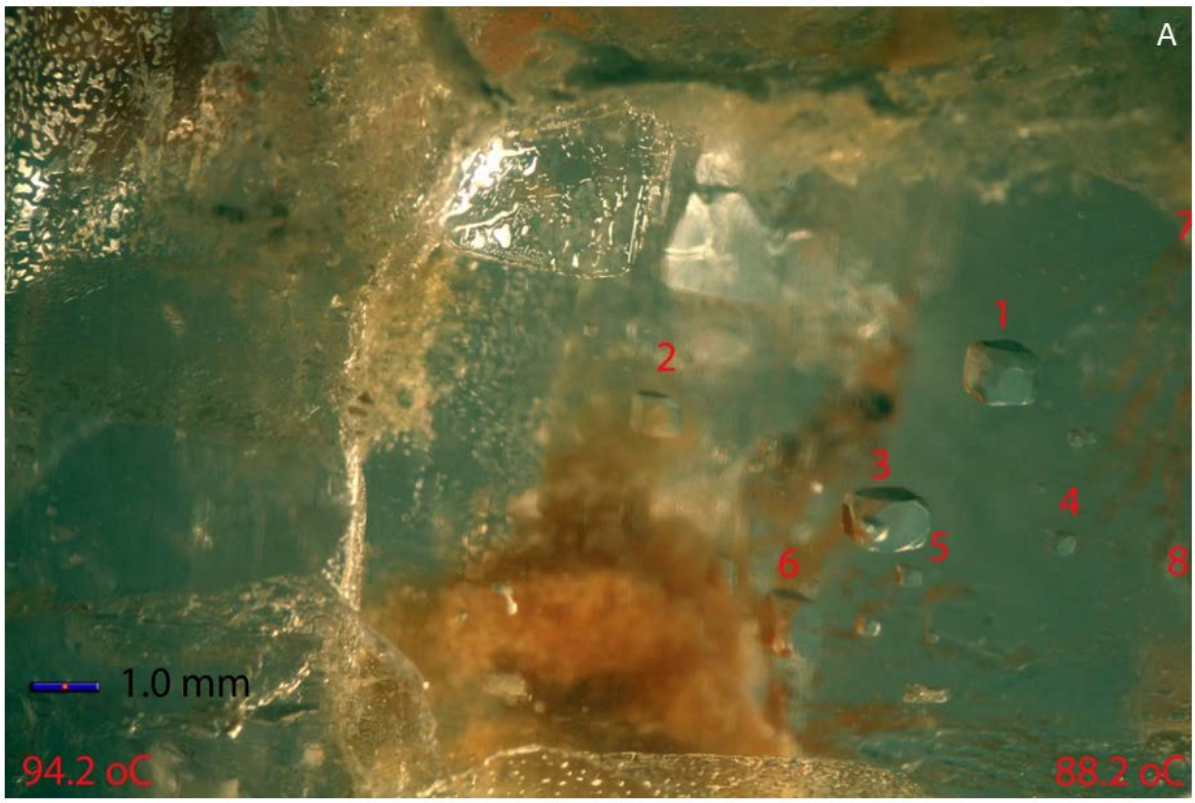

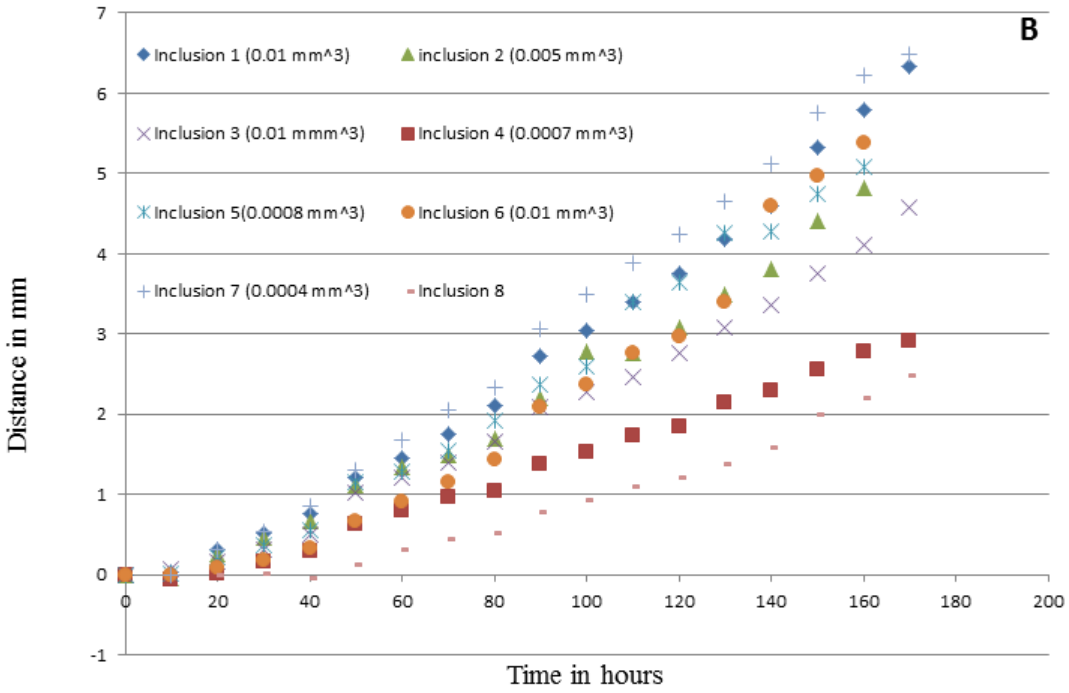

Figure 20. A) Inclusions 1 through 8 are labeled. B) Data showing migration distances of brine inclusions in a multi-crystalline salt sample. Temperature gradient in the domain recorded is 10 ^{o}C/cm. Maximum temperature 94 ^{o}C.

3.4.2 Brine migration in multi-crystalline salt with accessory mineral and clay under a thermal gradient

Measurements were performed on multi-grain salt specimens containing accessory minerals. The salt was mounted in the heating stage so that the clay minerals would intercept the migrating brine. Figure 21 shows the initial salt crystal before the start of the heating experiment and after heating for 76 hours. The temperature of the heating block was set at 190 ^{o}C. The temperature profile across the salt specimen is shown in Figure 22. The temperature profile observed is consistent will all previous measurements and indicates a fast decrease of temperature away from the heat source.

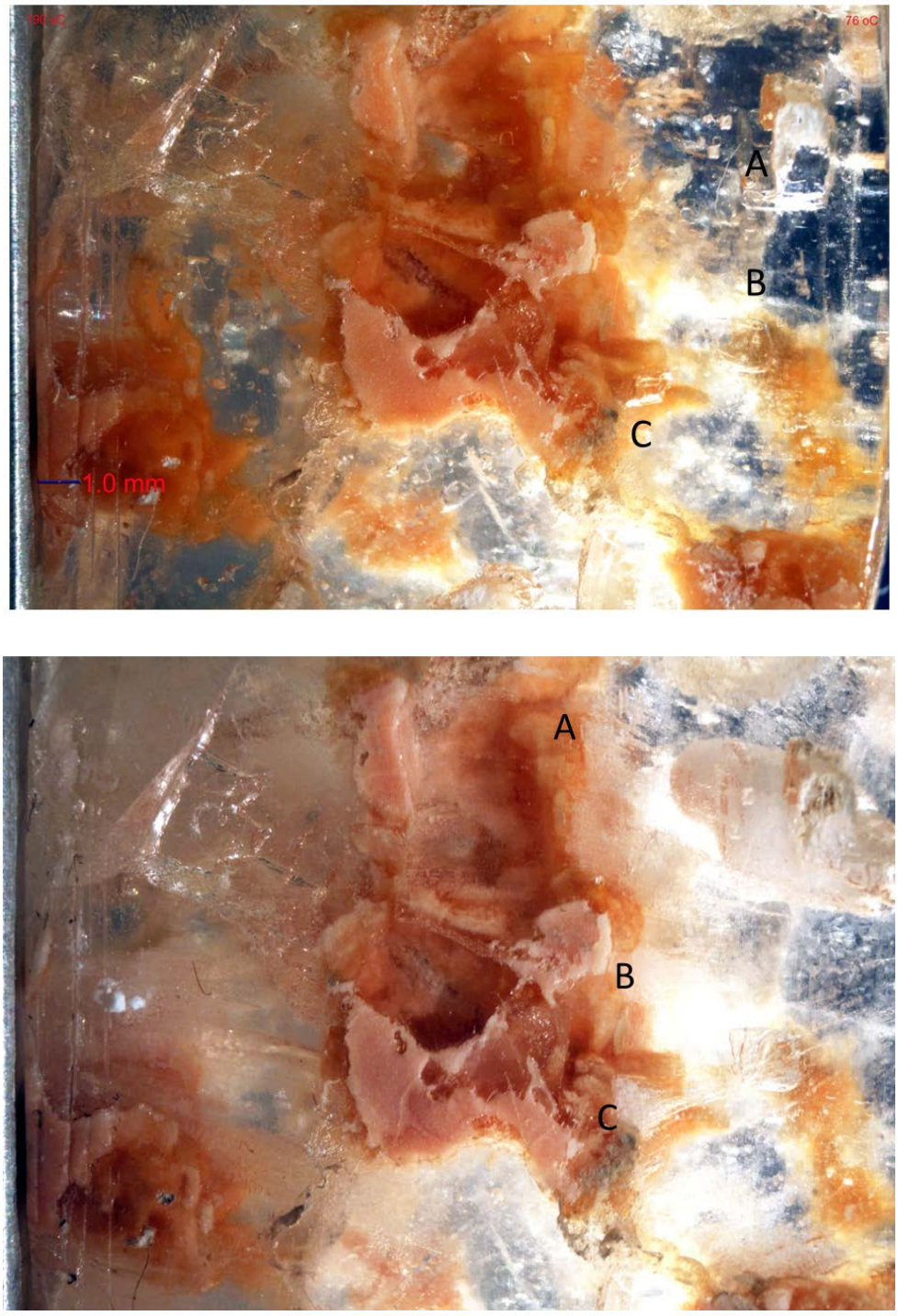

Figure 21. Clay impurities and brine inclusions in a salt sample before and after heating. The clay is the tan to reddish-brown material. The top photograph depicts the initial conditions. The bottom photograph was taken after 76 hours heating subjected to the temperature gradient detailed in Figure 22. Note that brine inclusions intercepting clay (example: A,B,C) stop migrating at the clay interface.

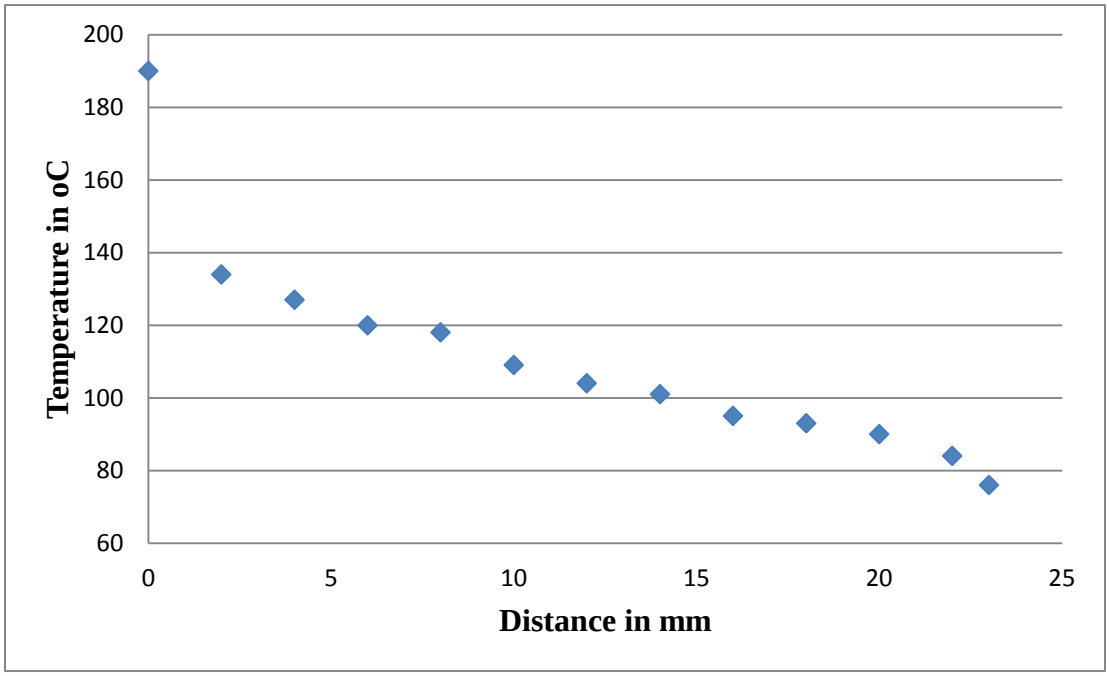

Figure 22. Plot of temperature gradient in a multigrain salt used to examine the effect of clay impurities on brine migration in salt: Salt dimensions: length: 2.3 cm, width 3.5 cm. Temperature of the heating block: 190 ^{o}C, temperature of the salt in contact with the heating block = 150 ^{o}C, Temperature of the room = 25 ^{o}C. Temperature at the cold side of the salt = 76 ^{o}C.

The important information gained from this experiment pertains to the behavior of brine at the clay interface. Our data clearly show that brine transport stops when it intercepts a clay impurity. More importantly we do not observe any moisture release from the clay under the temperature regimes examined here. Clay impurities at point A, B, C in the salt specimen are heated to 103 ^{o}C, 105 ^{o}C, and 100 ^{o}C respectively. At these temperatures we expect clay to lose a significant amount of hydration water (Caporuscio et al. 2013). We have shown in our previous report that impurities contained in salt examine here were dominated by clay, which loses its hydration water quickly when heated to 65-75 ^{o}C. These preliminary results do suggest that clay impurities in salt will play a significant role in controlling moisture transport under temperature gradients. They also show that clay contained in salt will become progressively saturated as it accumulates

more moisture. The retention of brine in the clay inclusions may be due to the confining pressure of the surrounding salt. This statement is conjecture at present. The changes will in turn change the mechanical properties of clay and affect the behavior of the salt assembly. More efforts need to be dedicated to understanding the full capacity of clay impurities to act as a moisture barrier and it is implication on the thermo-mechanical behavior of rock salt.

3.5 Corrensite dehydration experiments

During the Brine migration studies of FY-13, Caporuscio et al. (2013), identified corrensite as the predominant clay species. This phase was first identified at WIPP by Krumhansl, et al. (1990). In last year's research, corrensite was discovered to dehydrate in the temperature interval between 25 ^{o}C and 100 ^{o}C. This was clearly indicated in Figure 23 by multiple peak shifts. The corrensite dehydration studies were performed using in situ XRD characterization performed with an environmental cell. Experiments run under saturated conditions at 300 ^{o}C, 150 bar indicate that no further dehydration occurred in the clay.

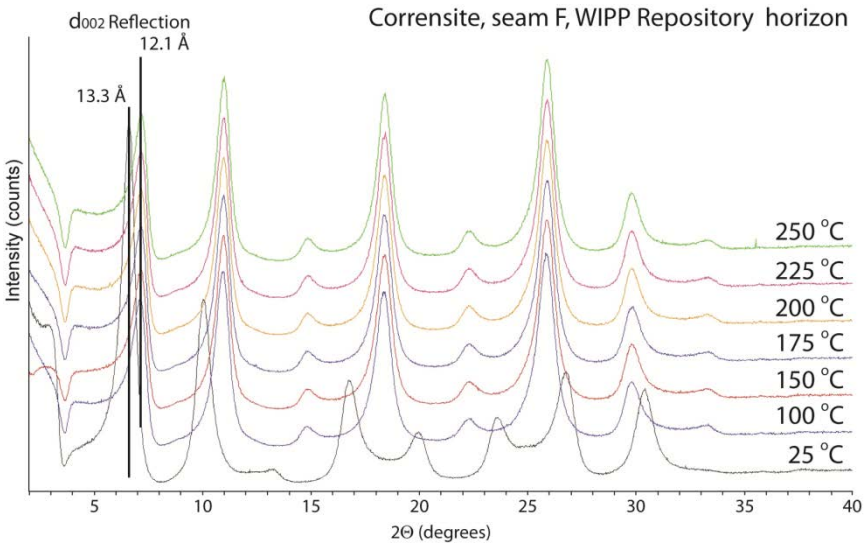

Figure 23. XRD spectra of corrensite from Seam F, at WIPP. Spectra measured at temperatures from 25 °C to 250 °C. Note especially the shift of the d0002 reflection that occurs from 25 °C to 100 °C. This indicates a loss of interlayer H_2O from the clay structure.

To narrow down the temperature of transition, further experiments were conducted on the heated stage XRD. Figure 24 shows the results of Corrensite heated stage XRD runs. Temperatures were from 25 °C to 100 °C at 10 °C intervals with RH ranging from 30 to 35%. There are two peak shifts, 13.7 to 12.3 Å and 9.1 to 8.6 Å, identified over the 75 °C range. This allowed us to conduct a final experiment in the temperature range 65 °C to 75 °C (Figure 25). The diffraction patterns for corrensite in Figure 25 indicate that there is a significant loss of interlayer water in the corrensite structure between 65 and 75 °C, as indicated by the peak shifts at 13.0 to 12.6 Å and 8.64 to 8.22 Å, respectively. By mapping the (001) d-spacing to temperature (Figure 26) one can see that there is a significant and rapid water loss between 65 and 75 °C. The interlayer water molecule site in corrensite is depicted in Figure 27. The chemical description of this dehydration is as follows:

$$(Ca, Na, K)(Mg,Fe,Al)_9(Si,Al)_8O_{20}(OH)_{10}9H_2O = (Ca,Na,K)(Mg,Fe,Al)_9(Si,Al)_8O_{20}(OH)_{10} + 9\ H_2O$$

The interlayer water dehydration process depicted above would release 13 wt. % water from stoichiometric corrensite. It must be stressed that this is a reversible process.

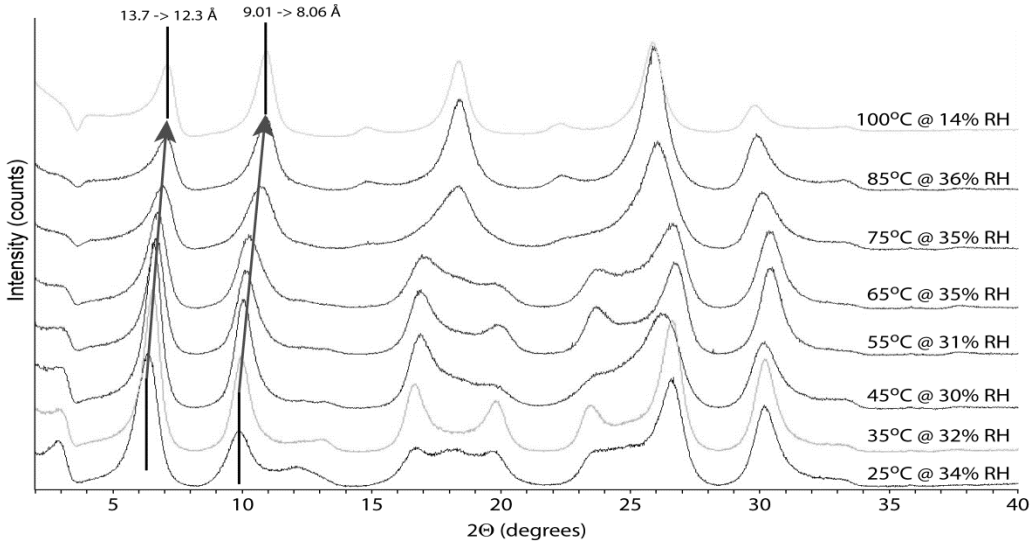

Figure 24. Corrensite XRD patterns from 25 to 100 ^{o}C. Note the two primary peak shifts at 13.7 to 12.3 Å and 9.1 to 8.6 Å.

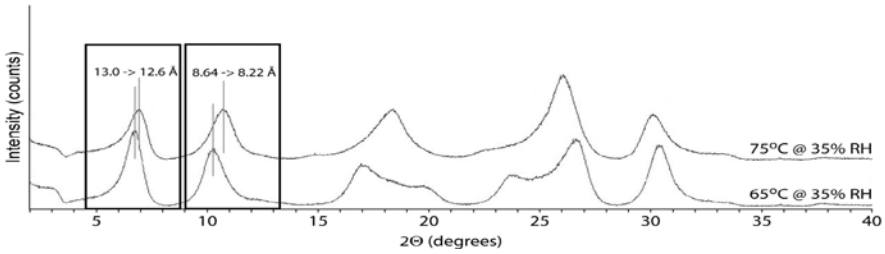

Figure 25. Corrensite 65- 75 C. XRD patterns at 35% RH. These are the most significant peak shifts at 13.0 to 12.6 Å and 8.64 to 8.22 Å, indicating a loss of interlayer water in the corrensite structure.

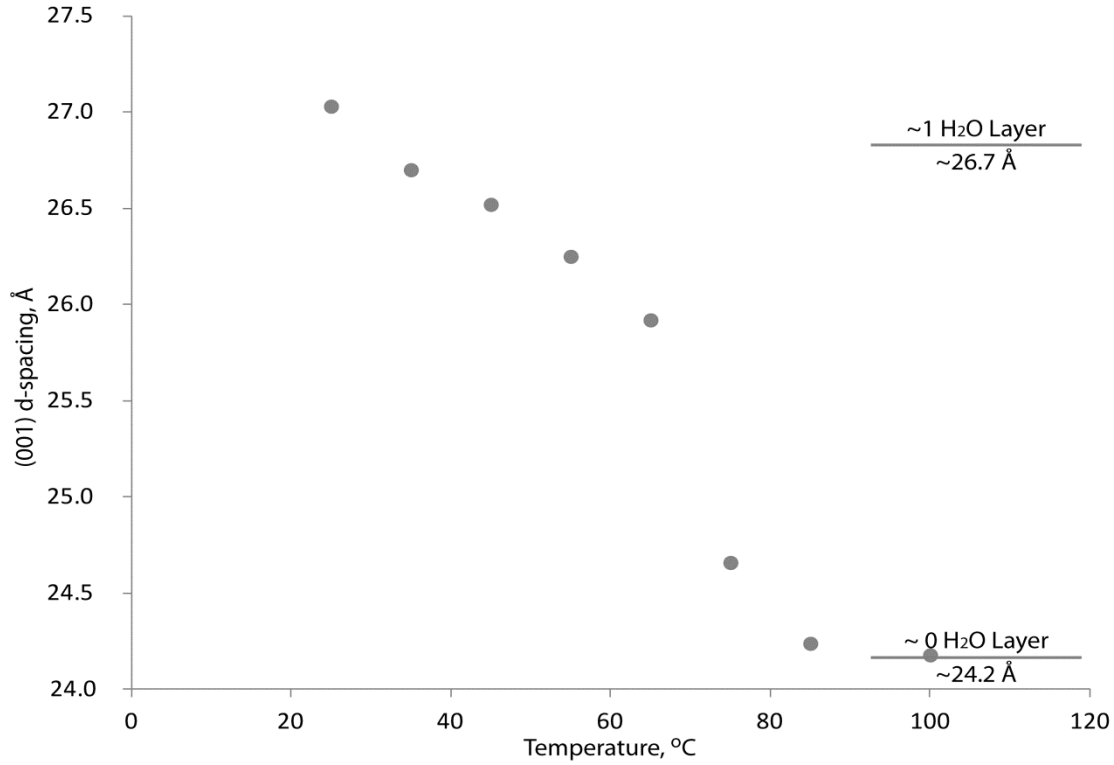

Figure 26. Corrensite dehydration as indicated by (001) d-spacing reduction.

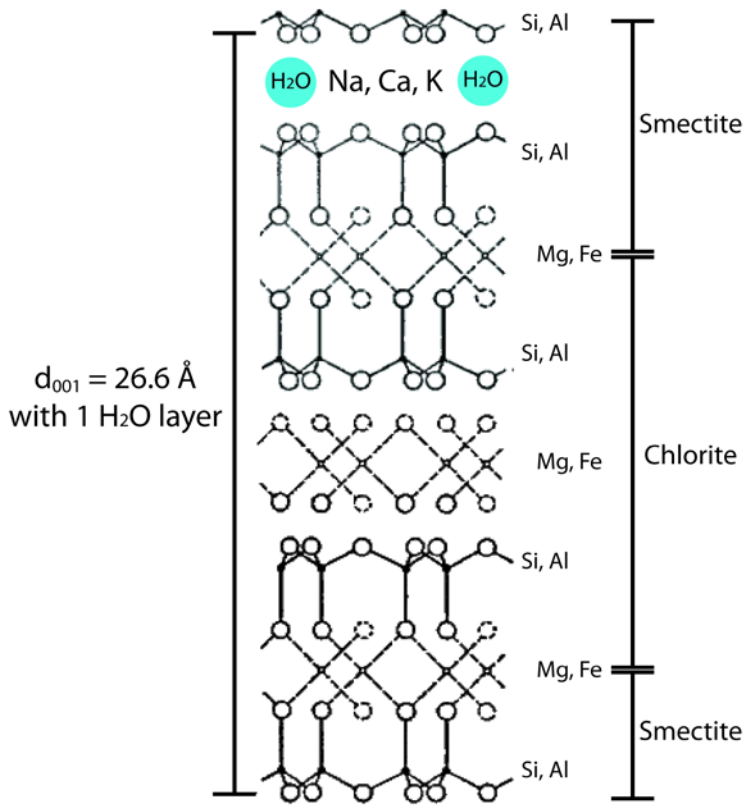

Figure 27. Stylized corrensite structure. The blue H_2O spheres indicate interlayer water.

The dehydration experiments described above are best summarized by the following paragraph as discussed by Caporuscio et al. (2013). "Lippmann (1976) presents a model of corrensite swelling where a fully dehydrated corrensite (above 200 ^{o}C) has a unit cell of 24 Å, the clay with interlayer water has a unit cell of 29 Å, and a fully saturated (i.e. moist) corrensite crystal has a unit cell of 33 Å. The author also indicates that the clay can hydrate – dehydrate reversibly and completely. It is this action that he attributes to the cause of floor heaves in tunnels in the Keuper Formation in Germany. Based on thermodynamic modeling, Vidale and Dubacq (2009) describe a similar hysteresis for smectites. The hydration – dehydration reversibly described holds true until there is a phase change at higher temperatures. Velde (1977) constructed phase

diagrams using experimental data to constrain the stability of illite-montmorillonite, corrensite, expanding chlorite, and illite. The author states that the Me^{3+} (i.e. Al^{3+} and/or Fe^{3+}) content of the assemblage, along with temperature and pressure constraints, will control whether an expanding chlorite or corrensite will appear. Using the diagrams produced by Velde (1977) corrensite, as sampled from WIPP, would have a large phase stability field under generic proposed repository conditions. Ryan and Hillier (2002) describe the co-existence of 3 layered phyllosilicates (berthierine/chamosite, corrensite, and chlorite) in evaporite associated facies of the Sundance Formation in Wyoming. Although the formation is predominantly sandstone, the clay rich facies give some insights into the formation and stability of the corrensite present. The authors state that the corrensite forms authigenically from saponite during burial diagenesis. They also discussed various lines of evidence to imply that the diagenetic conditions did not exceed 4000 m depth and 120 ^{o}C".

All evidence discussed indicates that corrensite is stable under present day conditions in the Salado Formation. The samples we collected were fully saturated and were shown to lose the interlayer water between 65 and 75 ^{o}C. From the discussion above, the corrensite clay should be able to rehydrate once temperatures drop below 65 ^{o}C (Wu et al., 1997).

High temperature stability reactions of corrensite in the presence of WIPP brine conducted this year provide the following information. A series of gold capsules were subjected to 300 ^{o}C, 160 bar conditions for a period of 6 weeks. Previous work (Caporuscio et al. 2013) provided information that corrensite was stable at these conditions in the presence of DI water. The present experiments determined any potential differences with WIPP brine waters (Molecke,

1983). Figure 28 shows the results of 4 corrensite + WIPP brine experiments. The brine contents vary from dry (0 wt. %) to 49 wt. % WIPP brine. All the samples with brine have identical 2Θ peak positions and intensities. Note that the dry sample has a slight positive shift at approximately 3 2Θ. This is probably due to the thickness of the sample and not due to clay structural changes.

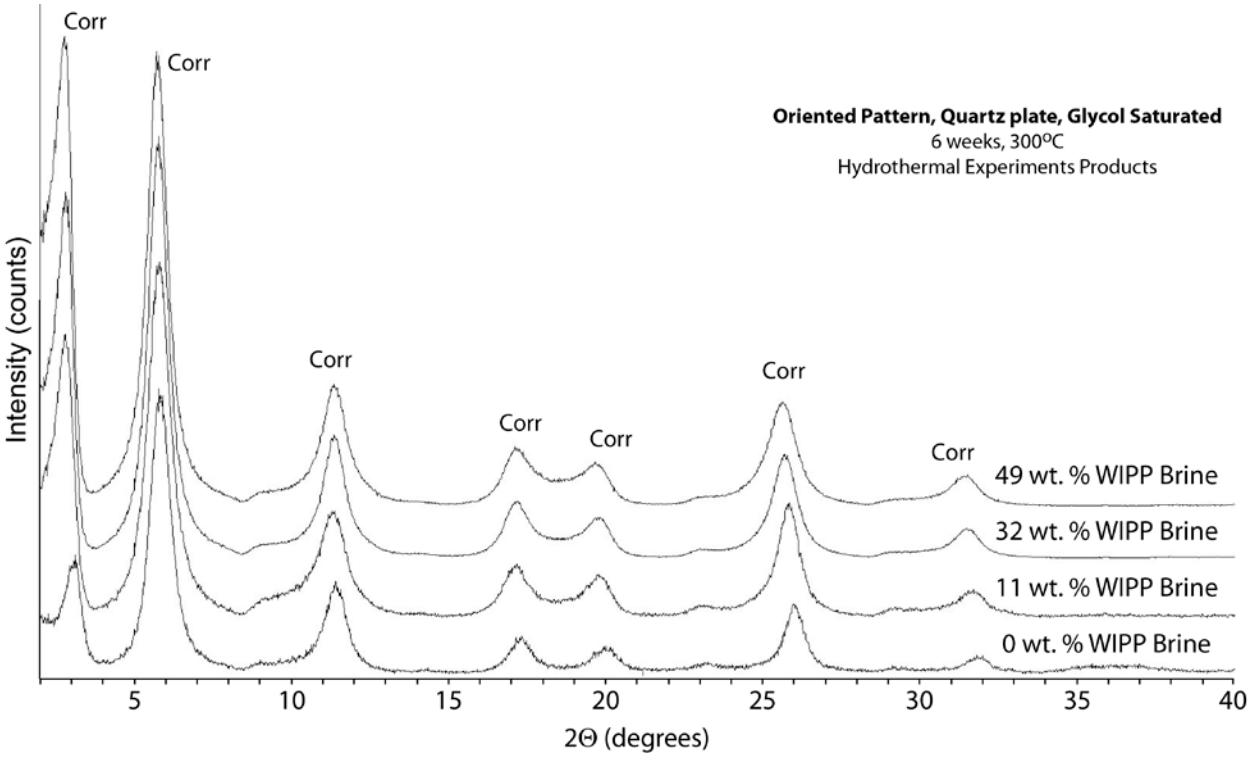

Figure 28. XRD spectra of high temperature corrensite + WIPP brine experiments. The spectra indicate that corrensite is stable at 300 ^{o}C, 160 bar under dry conditions and in the presence of various WIPP brine proportions.

However two variables are presently unknown. First, will hydration occur in a clay rich bed under lithostatic pressure conditions after closure of a repository? Second, will there be free

water available to rehydrate the clays? We believe these are important factors that deserve further research.

3.6 Sulfate dehydration investigations

Research completed in 2013 (Caporuscio et al. 2013) indicate that gypsum will transform to bassanite in the temperature range 50 to 75 ^{o}C and that gypsum is totally converted by 100 ^{o}C (Figure 29) .

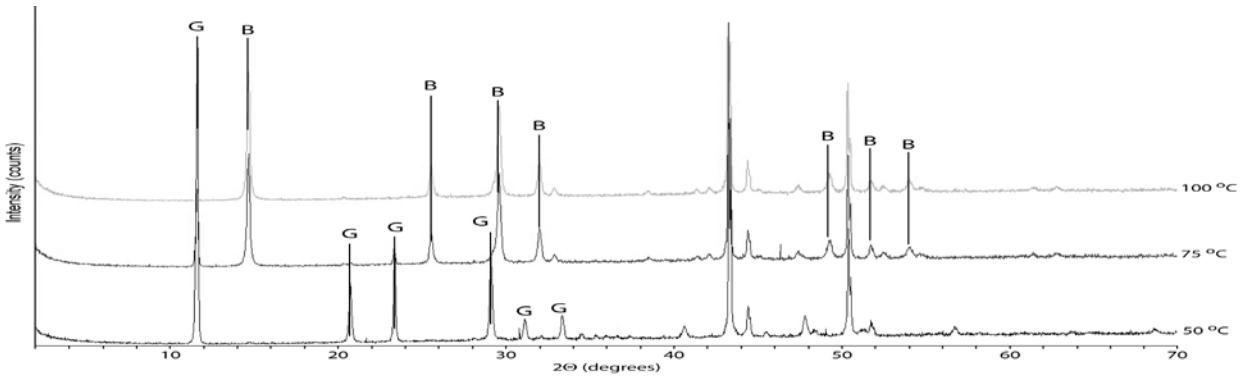

Figure 29. X-ray diffraction patterns showing the Gypsum to Bassanite transformation in situ by heating Naica gypsum samples at 50, 75, and– 100 ^{o}C.

The purpose of the following two experiments is to determine the stability of the phase transformations of the following sulfates at low temperatures.

($CaSO_4$ 2H_2O) → ($CaSO_4$ 0.5H_2O) + 1.5 H2O → ($CaSO_4$) + 0.5 H2O

Gypsum → Bassanite → Anhydrite

Figure 30 examines isothermal reactions at 70 ^{o}C using the XRD heated stage. The dehydration of the gypsum phase occurs rapidly, beginning at less than 17 hours. Bassanite is the

predominant phase that forms first, along with minor gamma anhydrite. After 50 more hours, gamma anhydrite becomes the predominant (and stable) sulfate phase. At 80 hours in the experiment, gamma anhydrite comprises approximately 90 volume percent of the sample. From 80 to 100 hours (end of experiment), approximately 10 volume % remnant bassanite still exists as a metastable phase.

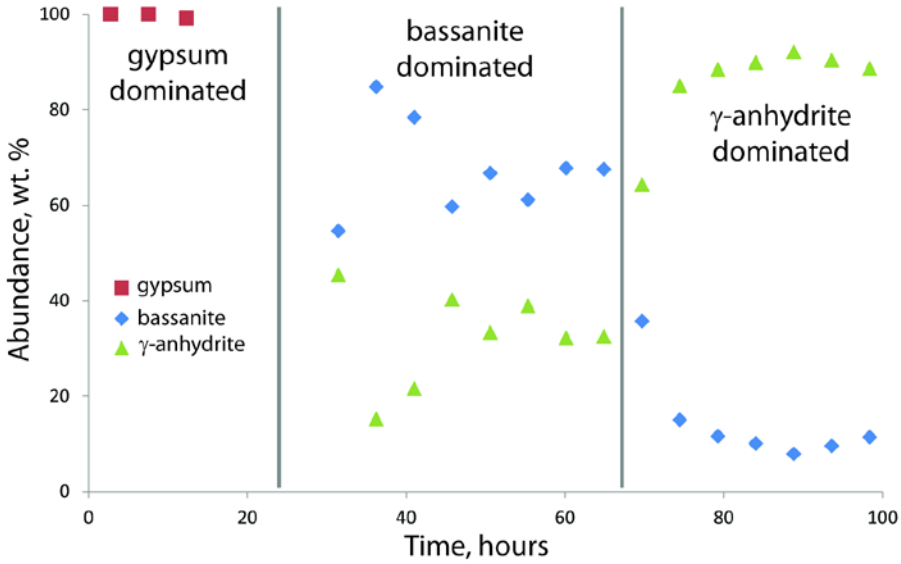

Figure 30. Isothermal, 70°C – Gypsum dehydration experiment. Note dominant formation of bassanite at early time, with minor amounts of gamma anhydrite. Gamma anhydrite becoming predominant at approximately 67 hours.

The second experiment examines the effect of salt in contact with gypsum. Figure 31 depicts the reaction of gypsum and salt in an isothermal reaction at 70 °C. The solid phases were combined in a 1:1 mixture. The experiment is a proof of concept to mimic the sulfate beds below the floor of the repository at WIPP. The dominant effect that is exhibited is that the addition of salt retards the co-formation of gamma anhydrite in the presence of bassanite. In Figure 30 both bassanite and gamma anhydrite began to form at less than 20 hours. However in this experiment, bassanite

forms as the sole phase at early times and gamma anhydrite only starts to replace bassanite beginning at 79 hours.

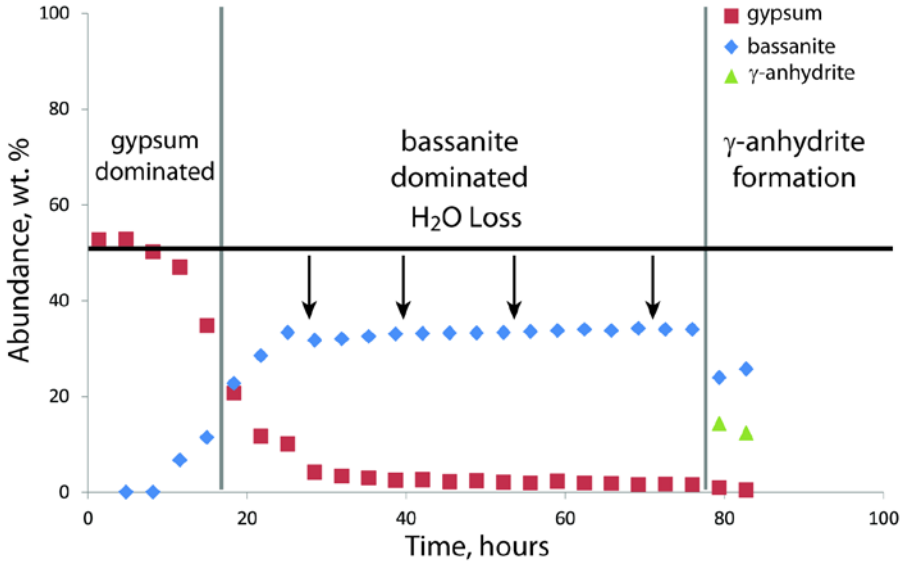

Figure 31. Isothermal, 70°C – Gypsum + WIPP Salt (1:1 mixture) dehydration experiment. In this experiment, containing equal amounts of sulfate and salt, bassanite is the only dehydration phase to initially occur. Gamma anhydrite first appears at approximately 79 hours in the reaction.

Therefore, the second experiment indicates that salt slows the dehydration transition from bassanite to anhydrite. One possibility is that salt is restricting heat flow in the sample. Regardless, the experiment shows that the H_2O loss produces a non 1:1 mixture.

A third set of experiments were prepared to determine the stability of sulfates at 300 °C, 160 bar in the presence of WIPP brine. Table 2 describes the experimental components and the unit cell refinements of the precursor gypsum and the resulting run products (gypsum and anhydrite). The individual experiments were 1) dry gypsum, 2) gypsum + 11wt. % WIPP brine and 3) gypsum + 32 wt. % WIPP brine. The run products were dominated by anhydrous anhydrite (averaging 94 wt. % of the resultant charge) with minor remnant gypsum (Figure 32). The anhydrous anhydrite

form indicates that even with the addition of excess water, the anhydrite will not revert to bassanite or gypsum at low temperatures. The cell parameters for pre-experiment and post reaction gypsum are essentially identical (unit cell lengths and angles). All the unit cell parameters for the anhydrous anhydrite products are also consistent between runs. These three experiments provide evidence that when gypsum is subjected to WIPP brine at hot repository conditions (300 ^{o}C, 160 bar); the resulting stable mineral phase is anhydrous anhydrite.

Table 2. Unit cell parameters of sulfates at 300 ^{o}C, 160 bar in the presence of WIPP brine. The run conditions are listed in column 1, run product percentages are listed in columns 2 and 3, gypsum cell parameters are listed in columns 4-9, anhydrous anhydrite cell parameters are listed in columns 10-15.

						GYP					ANH			
	Gypsum, wt. %	**Anhydrite, wt. %**	**a(Å)**	**b (Å)**	**c(Å)**	**α(°)**	**β (°)**	**γ(°)**	a (Å)	b (Å)	c (Å)	α(°)	β(°)	γ(°)
pre test	100	0	**6.29**	**15.24**	**6.53**	**90**	**127.5)**	**90**						
0 % Brine	5	95	**6.28**	**15.22**	**6.53**	**90**	**127.5**	**90**	7.002	7.00	6.241	90	90	90
11 % Brine	9	91	**6.23**	**15.19**	**6.54**	**90**	**127.6**	**90**	6.996	6.99	6.225	90	90	90
32 % Brine	3	97	**6.35**	**15.26**	**6.54**	**90**	**127.6**	**90**	6.997	6.99	6.24	90	90	90

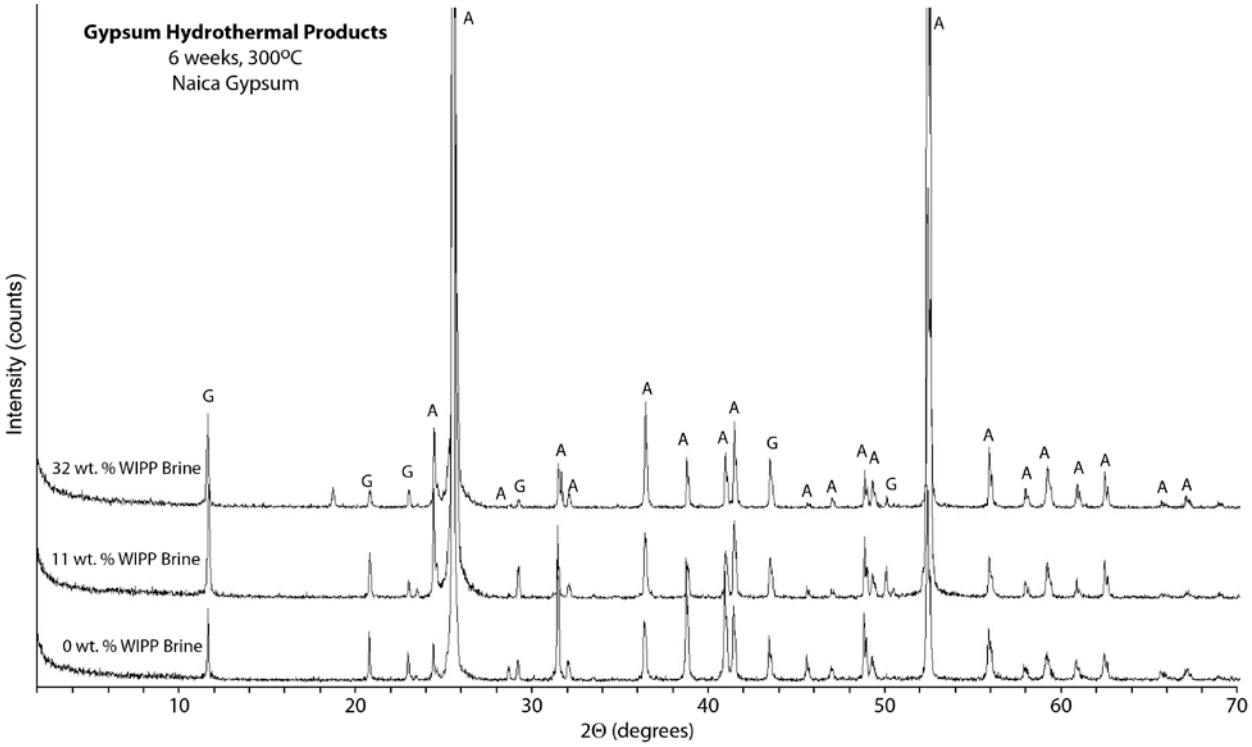

Figure 32. XRD spectra of gypsum plus WIPP brine experiments at 300 ^{o}C, 160 bar. Note that the stable phase in all three experiments (0 wt. % to 32 wt. % brine) is anhydrous anhydrite. Remnant metastable gypsum can be seen in all analyses. The extreme primary peak height of the anhydrite may be due to preferred crystal orientation on the slides.

Our experiments have determined that single phase vs multiphase reactions provide for different times of mineral transformation. The gypsum to bassanite phase transition at 70 ^{o}C seems stable for both reactions and is in line with the 76 ^{o}C reaction determined by Freyer (2000). In addition, time, temperature and pressure all seem to be controlling factors affecting the stability of metastable bassanite (Shcherban and Shirokikh, 1971). Shcherban and Shirokikh (1971) described the bassanite to anhydrite transformation as occurring between 100 and 140 ^{o}C. Our results differ significantly when the variables are time and mineral proportions. With pure sulfates at 70 ^{o}C, gamma anhydrite starts to occur by 17 hours and dominates at 32 hours. For the mixed sulfate + salt reaction anhydrite begins to occur at 79 hours. The significant temperature

difference between our experiments and those of Shcherban and Shirokikh (1971) may be due to the time allowed for the reaction to occur, and/or the salt thermal properties slowing the reaction to anhydrite. Robertson and Bish (2013) determined that the bassanite to anhydrite transformation occurred at temperatures as low as 85 ^{o}C at PH_2O of 1300 Pascals. This temperature climbed slightly as the PH_2O declined. Once again, our results compare well with those of Robertson and Bish (2013) for the bassanite to anhydrite transition at relatively high RH. Our third experiment results indicate that anhydrous anhydrite is the only stable sulfate at 300 ^{o}C, 160 bar in the presence of WIPP composition brine. Robertson and Bish (2013) also stated that bassanite is completely unstable at very low RH, and that gypsum rehydration from bassanite only occurs at 100 % RH. The authors also commented that the dehydration reactions are sluggish due to kinetic factors, however, our results suggest otherwise. As seen by two years of experiments, determining the metastable bassanite field would be critical to understanding the water release timing and amounts in a high temperature repository setting.

4. CONCLUSIONS

The results from this examination of water content in run of mine salt and brine migration in intact multi-crystalline salt show that moisture content in salt is controlled by its clay content. The data also show that moisture release from salt is directly related to clay dehydration behavior. Brine inclusions in salt, which represent less than 0.5 wt. % of the total salt moisture, do migrate towards the heat source. Brine migration crosses grain boundaries unhindered. However, the presence of clay impurities in salt seems to stop the migration of brine. The

implications of moisture accumulation in clay and its potential effects on the salts properties are not known.

Clay dehydration experiments from Caporuscio et al. (2013) indicate that corrensite releases 5 to 13 wt. % interlayer water between 65-75 ^{o}C and is then stable in dehydrated form to at least 300 ^{o}C. This reaction is also fully reversible when temperature is below 65 ^{o}C and water is available for rehydration. High temperature (300 ^{o}C, 160 bar) experiments conducted this year determining corrensite and gypsum stability in the presence of WIPP brine provide the following results. Corrensite is stable at the repository conditions over a range from 0 wt. % to 49 wt. % WIPP brine. At these same high P, T conditions gypsum changes to a new mineral phase, anhydrous anhydrite.

Caporuscio et al. (2013) concluded that over that same temperature range (65-75^{o}C) the gypsum to bassanite phase dehydration transformation releases 15 wt. % water. Time dependent experiments this year also provide data that in a sulfate only system, gamma anhydrite forms concurrently with bassanite at early times (17hours). By 80 hours, gamma anhydrite becomes the dominant sulfate phase. In the sulfate –salt dehydration experiment, bassanite only transformation occurs early on. Gamma anhydrite does not crystallize until approximately 80 hours, and metastable bassanite still occurs. Determining the metastable bassanite field at various RH conditions would be critical to understanding the water release timing and amounts in a high temperature repository setting.

The characterization of different type of waters in salt (e.g., water in the forms of fluid inclusions, surface water present as grain-boundary fluids, and water bound within secondary

minerals, e.g., clay and gypsum), and their mobility and evolution as function of temperature are pertinent factors for salt repositories. This preliminary study suggests that IINS based FDS may become viable techniques offering insights of the nature of water in rock salt. It is well suited to fingerprint different types of waters in geological materials, e.g. structural water, bulk water, and surface water.

In combination with TGA, mineral dehydration experiments and in situ continuous XRD monitoring, dehydration experiments at elevated P, T conditions, IINS shows promise and could reveal explicit details for characterization and quantifications of water types in rock salt. Thus, further investigations in multi-staged phases and scales should be conducted.

Our preliminary data on the potential use of low-field NMR for the characterization of moisture content in salt is very promising. We were able to determine the water content of an intact salt core, which was slightly less than 2.0 %. More importantly we were able to determine the relaxation time of the water present in salt and determine if it is free or bound water. This is a very promising technique that could allow rapid and accurate determination of water content in salt and it distribution among the different water categories (intra-crystalline water, hydration water, etc.).

5. REFERENCES

Anthony, T.R. and Cline, H.E. 1971 “The thermomigration of liquid Droplets through solids” J. Appl. Phys. 42, 3380.

Anthony, T.R. and Cline, H.E. 1972 " The thermomigration of biphase Vapor-liquid droplets in solids" Acta Metall. 20, 247.

Bein, A; Hovorka, S.D.; Fisher, R.S.; Rodder E. 1991 "Fluid inclusions in bedded Permian halite, Palo Duro, Basin, Texas- Evidence for modification of seawater in evaporate Brine-pools and subsequent early diagenesis" Journal of Sedimentary Petrology, Vol. 61(1):1-14.

Bradshaw, R.L. and W.C. McClain, Eds. 1971. "Project Salt Vault: A Demonstration of the Disposal of High-Activity Solidified Wastes in Underground Salt Mines." ORNL-4555. Oak Ridge, TN: Oak Ridge National Laboratory.

Braitsch, O, 1971 "Salt deposits their origin and composition" Springer-Verlag, New York, 297pp.

Caporuscio, F.A., Boukhalfa, H., Cheshire, M.C., Jorden, A.B., Ding, M. (2013) Brine Migration Studies for Salt Repositories. DOE Fuel Cycle Research and Development Document, FCRD-UFD-2013-000204

Carter, N.L., and Hansen, F.D. (1983) Creep of Rocksalt. Tectonophysics, V92, pp 275-333

Chipera, S.J. and Bish, D.L. (2002) FULLPAT: a full-pattern quantitative analysis program for X-ray powder diffraction using measured and calculated patterns. Journal of Applied Crystallography, 35, 744–749.

Freyer,D. 2000 Zur Phasenbildung und stabilitat im System Na_2SO_4 – $CaSO_4$ – H_2O. Dissertation , TU Bergakademie, Feiburg.

Freyer, D. and Voigt, W. (2003) Invited Review: Crystallization and Phase Stability of $CaSO_4$ and $CaSO_4$-Based Salts. Mon. fur Chemie 134, pp 693-719

Hohlfelder, J.J., 1979, " Measurement of water loss from Heated Geologic salt". SAND79-0462. Albuquerque, NM: Sandia National Laboratories.

Hohlfelder, J.J., 1981, "Volatile content of rock salt". SAND79-2349. Albuquerque, NM: Sandia National Laboratories.

Hohlfelder, J.J., McMurtry 1982, "Water content of brines contained in southeast New Mexico rock salt". SAND82-0530. Albuquerque, NM: Sandia National Laboratories.

Krause, W.B. 1983. "Avery Island Brine Migration Tests: Installation, Operation, Data Collection, and Analysis." ONWI-190(4). Columbus, Ohio: Battelle Project Management Division, Office of Nuclear Waste Isolation.

Krumhansl, J.L., Kimball, K. M. and Stein, C.L. 1990, "A review of WIPP repository Clays and their relationship to Clays of adjacent strata" SAN-90-0549. Sandia, National, Laboratory, Albuquerque, NM.

Kopp, O. C., and Combs, D. W., 1975, "Mineral sources of water in evaporite sequences (Salado salt and adjacent beds at the proposed waste disposal facility near Carlsbad in Lea and Eddy Counties, New Mexico)". Oak Ridge National Laboratory, Final Report, ORNL/SUB-3670-3-4, 34 p.

Line C.M.B. and Kearley G.J., 2000, An inelastic incoherent neutron scattering study of water in small-pored zeolites and other water-bearing minerals, J. Chem. Phy., 112 (20), 9058-9067.

Lippmann, F. (1976) "Corrensite, a swelling clay mineral, and its influence on floor heave in tunnels in the Keuper Formation". Eng. Geol., V 13, pp 65-70

Machiels, A.J.; Yagnik, S.; Olander, D.R.; Kohli, and R. 1981, "The mechanism of intragranular migration of brine inclusions in salt" Transaction of the American Nuclear Society, Vol.38: 169-170.

Molecke, M.A. 1983. *A Comparison of Brines Relevant to Nuclear Waste Experimentation.* SAND83-0516. Albuquerque, NM: Sandia National Laboratories.

Nowak, E.J. 1986. "Preliminary Results of Brine Migration Studies in the Waste Isolation Pilot Plant (WIPP)." SAND86-0720. Albuquerque, NM: Sandia National Laboratories.

Nowak, E.J., and D.F. McTigue. 1987. "Interim Results of Brine Transport Studies in the Waste Isolation Pilot Plant (WIPP)." SAND87-0880. Albuquerque, NM: Sandia National Laboratories.

Olander, D.R.; Machiels, A.J.; Balooch, M.; Muchowski, E.; Yagnik, S.K." Thermomigration of brine inclusions in sodium chloride single crystals" Trans. Am. Nucl. Soc.; 1980, Volume: 34: 352-353.

Olander, D.R.; Machiels, A.J.; Yagnik, S.K. 1981a, "Thermomigration of two-phase inclusions in salt" Trans. Am. Nucl. Soc.;, Volume: 35: 168-169.

Olander, D.R.; Machiels, A.J.; Muchowski, E.1981b, "Migration of Gas-liquid inclusions in single crystals of potassium and sodium chlorides" Nuclear Science and Engeneering, Vol.79(2): 212-227.

Popielak, R.S., R.L. Beauheim, S.R. Black, W.E. Coons, C.T. Ellingson and R.L. Olsen., 1983, "Brine Reservoirs in the Castile Formation, Waste Isolation Pilot Plant Project, Southeastern New Mexico" TME 3153. Carlsbad, NM: U.S. Department of Energy WIPP Project Office.

Powers, W. D., Lambert, J. S., Shaffer, S., Hill, R. L., Weart, D. W. Editors. 1978 "Geological characterization report, Waste Isolation Pilot Plant (WIPP) Site, Southern New Mexico", SAND78-1596 (Albuquerque, NM: Sandia Laboratories)

Robertson, K., and Bish, D. (2013) Constraints on the distribution of $CaSO_4\_nH_2O$ phases on Mars and implications for their contribution to the hydrological cycle. Icarus, V223, pp 407-417

Roedder, N. and Belkin H.E.,1980, "Migration of fluid inclusions in polycrystalline salt under thermal gradients", in Proc. of the 1980 NWS Progr. Info. Mtg., 0NWI-212, p 361.

Roedder, E.; Bassett, R. L., 1981, "Problems in determination of the water content of rock-salt samples and its significance in nuclear-waste storage siting". *Geology*. Vol. 9(11):525-350.

Rothfuchs, T., K. Wieczorek, H.K. Feddersen, G. Staupendahl, A.J. Coyle, H. Kalia, and J. Eckert. 1988. "Brine Migration Test: Asse Salt Mine, Federal Republic of Germany. Final Report." GSF-Bericht 6/88. Munich, Germany: Society for Radiation and Environmental Research.

Ryan P.C., and Hillier, S. (2002) Berthierine/chamosite, corrensite, and discrete chlorite from evolved verdine and evaporite-associated facies in the Jurassic Sundance Formation, Wyoming. Am Min, V87, pp 1607-1615

Shcherban, J.P., and Shirokikh, I.N. (1971) Thermodynamic and experimental data on Stability of gypsum, hennhydrate, and anhydrite under hydrothermal conditions. Int. Geology Review, 13: 11, pp 1671-1673.

Shefelbine, H. C., 1982, "Brine migration in salt: A summary report". SAND82-0152. Albuquerque, NM: Sandia National Laboratories.

Smyth, J.R., and Bish, D. 1988 "*Crystal Structures and Cation Sites of the Rock-Forming Minerals*" Allen & Unwin.

Stewart, F. H., 1963, "Marine evaporites: U.S. Geological Survey Professional Paper 440Y, 52 p.

Sugimoto, K., Dinnebier R. E. and Hanson J. C. 2007. "Structures of three dehydration products of bischofite from in situ synchrotron powder diffraction data (MgCl2·nH2O; n = 1, 2, 4)". Acta Cryst. 2007, B63, 235-242

Urai J.L., C.J. Spiers, H.J. Zwart, G.S. Lister, 1986, Weakening of rock salt by water during long-term creep, Nature, Vol. 324, 554-557.

Velde, B. (1977) A proposed phase diagram for illite, expanding chlorite, corrensite and illite-montmorillonite mixed layered minerals. Clays Clay Min. V25, pp 264-270

Vidal, O., and Dubacq, B. (2009) Thermodynamic modelling of clay dehydration, stability and compositional evolution with temperature, pressure and H2O activity. Geo. Cosmo. Acta., V73, pp 6544-6564.

Vista-Clara, Inc. http://www.vista-clara.com/instruments/corona/

Wu, T.C., Bassett, W., Huang, W.L., Guggenheim, S., and Koster Van Groos, A.F. 1997 "Montmorillonite under High H_2O pressures: Stability of Hydrate Phases, Rehydration Hysteresis, and the Effect of Interlayer Cations." Am. Min., Vol. 82, p. 69-78.

Yagnik, S.K. 1982 "Thermal gradient migration of brine inclusions in salt" Western Regional American Nuclear Society Student Conference, Oregon State University, Corvallis, OR, March 28-30, 1982. LNL-14080

Yagnik, S.K. 1983, " Interfacial stability of migrating brine inclusions in alkali-halide single-crystals supporting a temperature-gradient" Journal of crystal Growth, Vol. 62(3): 612-626.